Astron. Astrophys. 332, 410–428 (1998)

ASTRONOMY
AND
ASTROPHYSICS

Evidence for very large-scale coherent orientations of quasar polarization vectors⋆,⋆⋆

D. Hutsemékers⋆⋆⋆

Institut d'Astrophysique, Université de Liège, 5 av. de Cointe, B-4000 Liège, Belgium

Received 21 July 1997 / Accepted 17 December 1997

Abstract. On the basis of a new sample of quasar optical polarization measurements, we have found that, in a region of the sky, the quasar polarization vectors are not randomly oriented as naturally expected, but appear concentrated around one preferential direction.

In order to verify this surprising although preliminary result, we have compiled a large sample of quasar polarization measurements from the literature. With quite severe criteria to eliminate at best the contamination by our Galaxy, a sample of 170 quasars with good quality polarization measurements has been defined. Maps in redshift slices reveal a few regions where the polarization vectors are apparently aligned. To handle the problem more quantitatively, non-parametric 3D statistical tests were designed, as well as a method for visualizing spatially the results. The significance is evaluated through Monte-Carlo simulations.

Applied to our sample of 170 polarized quasars, two different statistical tests provide evidence, with significance levels of 0.005 and 0.015 respectively, that the optical polarization vectors of quasars are not randomly distributed over the sky but are coherently oriented on very large spatial scales. This orientation effect appears spatially delimited in the 3D Universe, mainly occuring in a few groups of 10-20 objects. The polarization vectors of objects located along the same line of sight but at different redshifts do not appear accordingly aligned. Essentially for this reason, instrumental bias and contamination by interstellar polarization in our Galaxy are unlikely to be responsible for the observed effect.

The very large scale at which this local orientation effect is observed indicates the presence of correlations in objects or fields on spatial scales $\sim 1000\,h^{-1}$ Mpc at redshifts $z \simeq$ 1-2, suggesting an effect of cosmological importance. Several possible and testable interpretations are discussed.

Key words: large-scale structure of the Universe – quasars: general – polarization – methods: statistical

1. Introduction

In the framework of a study of polarization properties of broad absorption line quasars, we have recently obtained new optical polarization measurements for a sample of moderate to high-redshift quasars (Hutsemékers et al. 1998). Significantly polarized objects were found. During the analysis of the data, we realized that in some regions of the sky the quasar polarization position angles are apparently not randomly distributed within 180° as naturally expected, but appear concentrated around one direction. Moreover, it was possible to delineate a contiguous volume in the three-dimensional space in which all objects have their polarization position angles within 80°. Although we are dealing with small numbers, the probability of such a situation is already small, but not meaningful since one may have picked out a peculiar configuration out of a random process. It nevertheless prompted us to see in the literature how the polarization position angles are distributed for quasars located in the same volume of the Universe. Five additional polarized quasars were found in the specified region, with the surprising result that their polarization position angles are concentrated around the same direction, giving a first evidence for some kind of coherent orientation on very large spatial scales. These preliminary results motivated us to carry out a more detailed statistical study of the distribution of quasar polarization position angles, using a sample, as large as possible, of measurements compiled from the literature.

In Sect. 2, we report in more detail the first evidence for spatially coherent orientations of quasar polarization vectors. In Sect. 3, we discuss the selection of a large sample of optical polarization measurements from data available in the literature. A preliminary analysis is given in Sect. 4, where we also

Send offprint requests to: D. Hutsemékers

⋆ Tables 2 and 3 are also available in electronic form at the CDS via anonymous ftp to cdsarc.u-strasbg.fr (130.79.128.5) or via http://cdsweb.u-strasbg.fr/Abstract.html

⋆⋆ Based in part on observations collected at the European Southern Observatory (ESO, La Silla)

⋆⋆⋆ Also, Chercheur Qualifié au Fonds National de la Recherche Scientifique (FNRS Belgium)

present maps of quasar polarization vectors in redshift slices. Since a quantitative statistical method is needed, we propose in Sect. 5 dedicated non-parametric statistical tests, together with a method for visualizing the results. Basically the tests measure the circular dispersion of polarization position angles for groups of neighbours in the three-dimensional space, the significance being evaluated through Monte-Carlo simulations. The results of the statistical tests are given in Sect. 6, providing evidence for polarization vector "alignments" on very large spatial scales. Since it is clear that the presence of such an effect may be of great importance for cosmology, some possible interpretations are discussed in Sect. 7, as well as possible biases in the data, the latter being essentially ruled out. Final conclusions form the last section.

2. First evidence from a small sample

With the aim of studying the polarization of broad absorption line (BAL) quasars, we have obtained optical linear polarization measurements for a sample of 42 moderate to high-redshift optically selected quasars. The observations were carried out at the European Southern Observatory (ESO) with the 3.6m telescope, during two runs in 1994. The telescope was equipped with the EFOSC camera set up in its imaging polarimetry mode (see e.g. di Serego Alighieri 1989). The details of these observations and their analysis are reported elsewhere (Hutsemékers et al. 1998).

Out of the 42 quasars, 20 were observed during the first observing run, all of them at high northern galactic latitudes b_{II}. 15 quasars appear significantly polarized, i.e. with $p \geq 2\,\sigma_p$, p denoting the measured degree of polarization (expressed in %), and σ_p the uncertainty. Since the uncertainties of these measurements are typically around 0.3%, this corresponds to values of p larger than 0.6 %, values from which one may consider the polarization to be intrinsic to the quasars (Berriman et al. 1990). This also corresponds to a maximum uncertainty $\sigma_\theta \simeq 14^\circ$ for the polarization angle θ[1], σ_θ being evaluated using the standard relation $\sigma_\theta = 28\overset{\circ}{.}65\ \sigma_p/p$ (e.g. Clarke & Stewart 1986).

While we naturally expect the quasar polarization angles to be randomly distributed between 0° and 180°, it appears that 11 out of the 15 polarized objects have their angles θ distributed within the limited range $\Delta\theta = 83^\circ$. More interestingly, we can define a contiguous volume in the three-dimensional (3D) space, limited by redshifts $z \leq 2.3$ and right ascensions $\alpha \geq 11^h\ 15^m$, where all the quasars, i.e. 7 objects, have their polarization angles between 146° and 46°, i.e. in the range $\Delta\theta = 80^\circ$ (cf. Table 1). The probability that such a situation occurs by chance is of the order of a few percent, but completely meaningless since evaluated *a posteriori*. However, if an orientation effect[2] is indeed present, these observations can be used to predict that, in the volume delimited in redshift and right ascension by our first set of 7 objects (i.e. $11^h15^m \leq \alpha \leq 14^h29^m$ and $1.465 \leq z \leq 2.222$) , every significantly polarized quasar should have a polarization angle between 146° and 46°. Assuming that the distribution of position angles is only due to chance, the probability to find n objects, different from those of the first set, within this angle range is simply $(80/180)^n$.

Table 1. The two quasar samples showing polarization vector alignments: the first, from our observations, suggesting the effect, and the second, from the literature, confirming it

Object	b_{II}	z	p	σ_p	θ	σ_θ	Ref
1115+080	+61	1.722	0.68	0.27	46	12	0
1120+019	+57	1.465	1.95	0.27	9	4	0
1212+147	+75	1.621	1.45	0.30	24	6	0
1246−057	+57	2.222	0.91	0.28	146	9	0
1309−056	+57	2.212	0.78	0.28	179	11	0
1331−011	+60	1.867	1.88	0.31	29	5	0
1429−008	+53	2.084	1.00	0.29	9	9	0
1222+228	+82	2.046	0.84	0.24	150	8	2
1246−057	+57	2.222	2.06	0.29	150	4	2
1255−316	+31	1.924	2.20	1.00	153	12	4
1303+308	+85	1.770	1.12	0.56	170	14	3
1309−216	+41	1.491	12.30	0.90	160	2	4
1309−056	+57	2.212	2.33	0.57	179	7	2
1354−152	+45	1.890	1.40	0.50	46	10	4

References: (0) Hutsemékers et al. 1998, (2) Stockman et al. 1984, (3) Moore & Stockman 1984, (4) Impey & Tapia 1990

To check this, we have compiled quasar optical polarization measurements from all major surveys available in the literature (see next section). Adopting the same quality requirements on the data, i.e. $\sigma_\theta \leq 14^\circ$and $p \geq 0.6\%$, 7 polarized objects are found in the volume previously defined in right ascension and redshift (cf. Table 1). Two objects (1246-057 and 1309-056) are common with our first set, and their published polarization angles are in excellent agreement with our measurements (the differences in the polarization degree p are most probably due to the fact that the measurements were not done in the same filters). It came as a surprise that all of the 5 remaining objects have angles within the range predicted from our first sample, a situation which has a probability of only 1.7% to occur by chance.

More confidence within this preliminary result can be gained from the fact that we had a priori no reason to fix the lower limit in z as in our first sample (except for being able to compute a probability *a priori*), and that if we adopt $z \geq 1.0$ instead of 1.465, 4 polarized objects (1127-145, 1246+377, 1254+047,

[1] The polarization position angle, or simply polarization angle, θ, is expressed in degrees from 0° to 180°, and counted from the north-south direction in the equatorial coordinate system, clockwise if east is to the right. Polarization *vectors* refer to non-oriented lines of arbitrary length centred at the object position with a direction fixed by the polarization angle

[2] It is important to note that throughout this paper we will speak of *alignments* or *coherent orientations*, although the polarization vectors are generally poorly aligned, i.e. for example when the polarization angles are distributed within 80-90°, instead of spanning 180° as expected from a uniform distribution

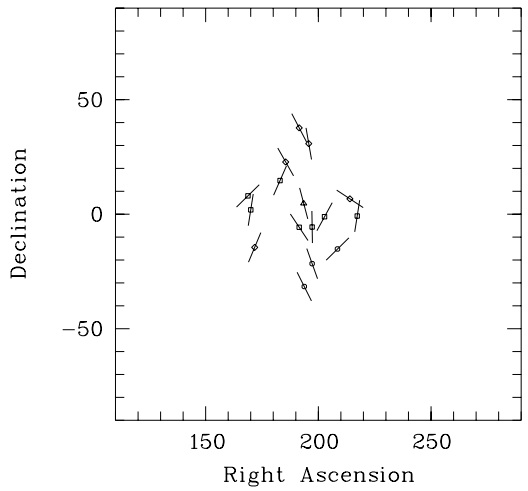

Fig. 1. A map of the polarization vectors of *all* polarized ($p \geq 0.6\%$ and $\sigma_\theta \leq 14^\circ$) quasars found in the literature with right ascensions $11^h15^m \leq \alpha \leq 14^h29^m$, and redshifts $1.0 \leq z \leq 2.3$ (i.e. the objects from Table 1, plus 4 additional ones mentionned in the text). The vector length is arbitrary. The different symbols refer to different catalogues: Stockman et al. 1984, and Moore & Stockman 1984 [losanges], Berriman et al. 1990 [triangles], Impey & Tapia 1990, and Impey et al. 1991 [circles], Hutsemékers et al. 1998 [squares]

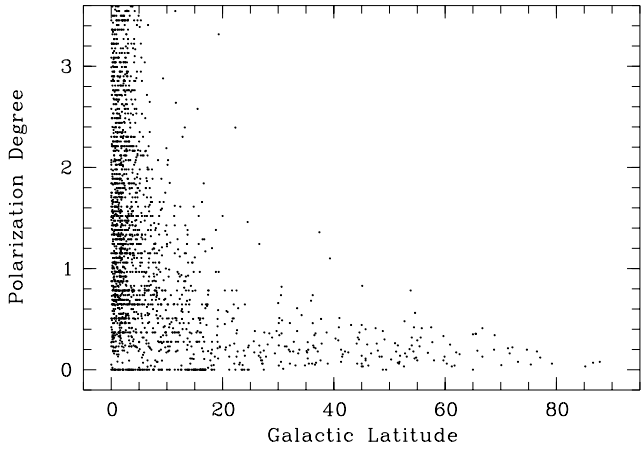

Fig. 2. The polarization degree (p in %) of distant ($d \geq 400$pc) stars of our Galaxy as a function of their galactic latitude $|b_{II}|$. All data are from the catalogue of Axon & Ellis (1976). The plot has been truncated to $p = 3.6\%$ to emphasize the behavior of low-polarization objects, while keeping all stars with $|b_{II}| \geq 20^\circ$

and 1416+067) may be added to the sample, 3 of them with polarization vectors accordingly aligned (cf. Tables 2 and 3). Also, if we plot on a map all the objects considered up to now (Fig. 1), a structure is apparent in the sense that the polarization vectors are better aligned at the centre of the group: all quasars with $12^h22^m \leq \alpha \leq 13^h09^m$ (i.e. 8 objects) have $146^\circ \leq \theta \leq 179^\circ$ ($\Delta\theta = 33^\circ$), suggesting a much more significant effect. It is clear from Fig. 1 that, if quasar polarization vectors are coherently oriented, this occurs on very large spatial scales.

These preliminary results provide a first, moderate, evidence for a coherent orientation effect of quasar polarization vectors in a limited, although very large, region of the sky. The fact that objects from different surveys, observed with different instrumentations, behave similarly indicates that the effect is unlikely to be due to an instrumental bias. These results motivate the construction of a larger sample from the literature to investigate if statistically significant alignments may be detected in other regions of the sky, therefore providing more definite evidence for the physical reality of the effect.

3. The selection of a large sample from the literature

In order to have a larger sample of quasar polarization angles, we have compiled optical polarization measurements from all (to our knowledge) major surveys available in the literature i.e. those by Stockman et al. (1984), Moore & Stockman (1984), Berriman et al. (1990), Impey & Tapia (1990), Impey et al. (1991), Wills et al. (1992), and Hutsemékers et al. (1998). Several of these surveys contain new measurements together with a compilation of data from the literature. Here, we only consider objects for which the polarization angle and the redshift are given, and which are classified by the authors as quasars. Seyfert galaxies and radio-galaxies were discarded, while BL Lac objects included by the authors in their quasar samples were taken into account, the BL Lac nature being not the primary criterion of selection. Note that some polarization surveys only dedicated to BL Lac objects may be found in the literature. These were not considered in our compilation, not only because the nature of BL Lac objects and their relation to quasars is still unclear, but also because their redshifts are uncertain (when measured), and because it is often difficult to assess a unique value to their polarization angle. When more than one measurement is available in a given catalogue, we have taken the data obtained with the lowest uncertainty σ_p, whatever the value of p, θ, σ_θ, the filter in which it was observed, or the possible or known variability. Measurements with the smallest σ_p were preferred to those with the smallest σ_θ since σ_θ depends on p and may be biased. Our sample finally amounts to 525 measurements which correspond to 433 different quasars, several objects belonging to more than one catalogue.

Due to the fact that this is always a positive quantity, the polarization degree p is biased at low signal to noise (e.g. Clarke & Stewart 1986). It is important to note that the polarization position angle is *not* affected by such a bias; only the uncertainty σ_θ may be biased when computed using the standard formula $\sigma_\theta = 28.^\circ65\ \sigma_p/p$, as done in most surveys. Since in most catalogues the polarization measurements were not corrected for bias, we only consider the measured values of p as they are reported. The values of σ_θ were also used as reported, except for the Wills et al. (1992) sample where the uncertainties are not given. For this sample, σ_θ was re-computed using the standard formula.

Our compilation contains polarization measurements obtained with various filters, and even in white light, which, due to the range in redshift, correspond to quite different spectral

regions in the quasar rest frame. Any wavelength dependence of the polarization angle would contribute to smear out coherent orientation effects. Fortunately, while the degree of polarization may depend on wavelength, the quasar polarization angles show apparently little or no wavelength dependence in the optical to near-infrared spectral range, a characteristics which seems common to low and high polarization objects, as well as to BAL quasars (cf. e.g. Saikia & Salter 1988, the multi-wavelength studies by Stockman et al. 1984, Webb et al. 1993, and the spectro-polarimetric observations by de Diego et al. 1994, Smith et al. 1994, Cohen et al. 1995). This important property seems to extend to the ultraviolet (Impey et al. 1995), although up to now very few objects have been observed. Also, the time variability of the polarization degree and the position angle, which is observed in many strong radio sources (e.g. Saikia & Salter 1988, Impey et al. 1991), will add some noise to the orientation effects. We nevertheless prefer to keep these objects in the sample because they have generally high, well measured polarization which can definitely not be attributed to extinction in our Galaxy. Furthermore, it seems that for many blazars, the polarization angles do not vary within a very large range of values, at least in the considered sample (Impey et al. 1991). While these effects certainly affect our data to some extent, we emphasize that they can only act to reduce the deviation from an uniform distribution, and certainly not to produce coherent orientations.

Although we want to keep as many quasars as possible, it is useless to consider objects for which the polarization angle measurements are too uncertain. We therefore adopt the reasonable constraint $\sigma_\theta \leq 14°$, which is equivalent to $p \geq 2\,\sigma_p$. It is important to remark that with this signal to noise ratio, the bias on p is not larger than $\sim 10\%$ (cf. Wardle & Kronberg 1974).

Further, it is necessary to reduce as much as possible the contamination by extinction in our Galaxy. This is especially important in our case since this mechanism is well known to align polarization vectors. On the basis of the Burstein & Heiles (1982) extinction maps, Berriman et al. (1990) have evaluated the contribution of the galactic interstellar medium to the polarization of their objects, which are essentially low-polarization quasars. They conclude that virtually any measured value of p above 0.6% is intrinsic to the quasar. A similar conclusion is reached in Hutsemékers et al. (1998), using polarization measurements of faint stars located in the immediate vicinity of the quasars. We will therefore adopt this necessary cut-off value and consider only objects with $p \geq 0.6\%$. It is clear that the highest the cut-off value, the lower contamination one can expect. But our sample is dominated by low-polarization quasars, the number of which precisely peaks near 0.6% (cf. Berriman et al. 1990), such that choosing a higher cut-off value would dramatically decrease the number of objects in our sample.

It is also necessary to discard objects at low galactic latitude, the usual choice being $|b_{II}| \geq 20°$. However, looking at the Burstein & Heiles (1982) maps, there is still significant extinction between 20° and 30°, especially in the southern part of the sky: $E_{B-V} \simeq 0.09$ is not unusual, which corresponds to $p_{ISM} \lesssim 0.75\%$ using the standard formula $p_{ISM} \leq 8.3\,E_{B-V}$ (Hiltner 1956). This indicates that a more stringent cut-off could be valuable. In Fig. 2, we have used the compilation by Axon & Ellis (1976) to plot the polarization degree of galactic stars as a function of their galactic latitude. Only distant stars ($d \geq 400$ pc) are considered i.e. those lying beyond the local volume where most interstellar polarization is imprinted. Here also, choosing $|b_{II}| \geq 30°$ rather than $|b_{II}| \geq 20°$ appears safer to have less galactic contamination above p = 0.6%. Adopting this more stringent cut-off decreases the number of objects in the sample, but the effect is not so dramatic, first because the quasar distribution peaks around $|b_{II}| \simeq 40°$ (cf. Fig. 3), and second because the considered volume of the Universe also decreases, such that the number of objects per unit volume, which is an important quantity in 3D investigations, is essentially unaffected.

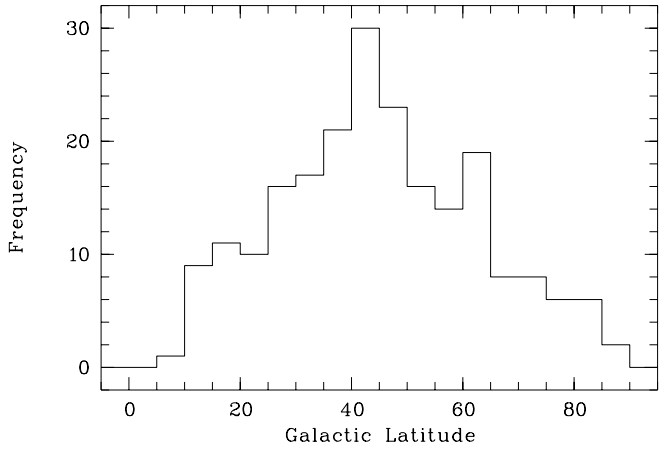

Fig. 3. The distribution in galactic latitude ($|b_{II}|$) of the quasars from our compilation. Only those objects with $p \geq 0.6\%$ and $\sigma_\theta \leq 14°$ are represented here

Finally, with the conditions $\sigma_\theta \leq 14°$, $p \geq 0.6\%$, $|b_{II}| \geq 30°$, and keeping only the best measurement when several are available (i.e. the ones with the smallest σ_p), our final sample amounts to 170 different polarized quasars. With the adopted constraints, we expect a priori little contamination by extinction in our Galaxy. The objects are given in Tables 2 and 3, with some of their characteristics. Note that the uncertainty of the polarization angle, σ_θ, is roughly uniformly distributed between 1° and 14°, and has therefore a mean value close to 7°.

4. Preliminary analysis of the sample

4.1. Are the polarization angles uniformly distributed?

We can test the hypothesis that the polarization angles in the final sample of 170 quasars are drawn from an uniform distribution using the Kuiper test (see e.g. Fisher 1993) which is similar to the well-known Kolmogorov-Smirnov test, but adapted to circular data. Due to the condition $|b_{II}| \geq 30°$, the objects lie in a biconical volume, whose northern and southern parts are essentially disconnected except at low redshift. We therefore consider subsamples at northern and southern galactic latitudes, and at low and high redshifts. The Kuiper test does not provide any ev-

Table 2. The final sample of 170 polarized quasars

Object	b_{II}	z	p	σ_p	θ	σ_θ	Ref
0003−066	−67	0.347	3.50	1.60	160	12	4
0003+158	−45	0.450	0.62	0.16	114	7	2
0013−004	−62	2.084	1.03	0.33	115	10	0
0017+154	−47	2.012	1.14	0.52	137	13	3
0019+011	−61	2.180	0.93	0.26	24	8	2
0021−022	−64	2.296	0.70	0.32	170	14	0
0024+224	−40	1.118	0.63	0.29	90	14	2
0029+002	−62	2.226	0.75	0.34	158	14	0
0050+124	−50	0.061	0.61	0.08	8	3	1
0051+291	−34	1.828	0.80	0.38	119	14	3
0059−275	−88	1.594	1.62	0.29	172	5	0
0100+130	−50	2.660	0.84	0.29	112	10	2
0106+013	−61	2.107	1.87	0.84	143	13	3
0110+297	−33	0.363	2.60	1.15	63	13	2
0117+213	−41	1.493	0.61	0.20	102	9	1
0119+041	−58	0.637	4.20	1.10	59	6	4
0123+257	−36	2.358	1.63	0.81	140	14	3
0130+242	−38	0.457	1.70	0.52	110	9	2
0133+207	−41	0.425	1.62	0.36	49	6	3
0137−018	−62	2.232	1.12	0.29	61	8	0
0137−010	−61	0.330	0.63	0.31	154	14	2
0145+042	−56	2.029	2.70	0.32	131	3	0
0146+017	−58	2.920	1.17	0.23	138	5	2
0148+090	−51	0.299	1.21	0.54	139	13	3
0159−117	−67	0.699	0.65	0.30	4	13	2
0202−172	−70	1.740	3.84	1.13	98	9	6
0205+024	−55	0.155	0.72	0.17	22	7	2
0208−512	−62	1.003	11.50	0.40	88	1	4
0214+108	−47	0.408	1.13	0.22	121	6	2
0226−038	−57	2.064	1.20	0.53	68	13	2
0232−042	−56	1.436	0.91	0.32	163	10	2
0332−403	−54	1.445	14.80	1.80	113	3	4
0333−380	−54	2.210	0.83	0.28	45	10	0
0336−019	−43	0.852	19.40	2.40	22	4	4
0348+061	−35	2.058	1.39	0.51	157	10	2
0350−073	−43	0.962	1.67	0.24	14	4	2
0402−362	−49	1.417	0.60	0.30	66	14	4
0403−132	−43	0.571	3.80	0.50	170	4	4
0405−123	−42	0.574	0.83	0.16	136	5	2
0414−060	−37	0.781	0.78	0.22	146	8	2
0420−014	−33	0.915	11.90	0.50	115	1	4
0438−436	−42	2.852	4.70	1.00	27	6	4
0451−282	−37	2.559	1.80	0.50	66	9	4
0454−234	−35	1.009	27.10	0.50	3	1	6
0506−612	−36	1.093	1.10	0.50	83	12	4
0537−441	−31	0.894	10.40	0.50	136	1	4
0804+499	+32	1.430	8.60	0.70	179	2	4
0836+710	+34	2.170	1.10	0.50	102	12	4
0839+187	+32	1.270	1.74	0.53	100	9	6
0844+349	+38	0.064	0.63	0.13	26	6	1
0848+163	+34	1.932	1.37	0.54	27	11	2
0850+140	+33	1.110	1.05	0.50	106	14	3
0851+202	+36	0.306	10.80	0.30	156	1	4
0855+143	+34	1.048	5.31	2.12	30	11	3
0903+175	+37	2.776	0.93	0.29	60	9	0
0906+430	+43	0.670	3.80	0.40	53	2	4
0906+484	+43	0.118	1.08	0.30	148	8	2
0923+392	+46	0.699	0.91	0.35	102	11	3
0946+301	+50	1.216	0.79	0.19	110	7	1
0953+254	+51	0.712	1.45	0.33	127	7	6
0954+556	+48	0.901	8.68	0.82	4	3	6
0954+658	+43	0.368	19.10	0.20	170	1	5
1001+054	+44	0.161	0.77	0.22	74	8	2
1004+130	+49	0.240	0.79	0.11	77	4	1
1009−028	+41	2.745	0.95	0.30	178	9	0
1011+091	+49	2.262	2.12	0.30	143	4	0
1012+008	+44	0.185	0.66	0.23	98	10	1
1029−014	+46	2.038	1.13	0.31	121	8	0
1038+064	+53	1.270	0.62	0.24	149	11	2
1048−090	+43	0.344	0.85	0.30	96	10	2
1049+616	+50	0.422	0.83	0.34	176	12	2
1055+018	+53	0.888	5.00	0.50	146	3	4
1100+772	+39	0.313	0.71	0.22	76	8	2
1114+445	+64	0.144	2.37	0.18	96	2	1
1115+080	+61	1.722	0.68	0.27	46	12	0
1120+019	+57	1.465	1.95	0.27	9	4	0
1127−145	+44	1.187	1.26	0.44	23	10	2
1128+315	+72	0.289	0.95	0.33	172	10	2
1151+117	+69	0.176	0.90	0.19	94	6	1
1156+295	+78	0.729	2.68	0.41	114	4	6
1208+322	+80	0.388	1.03	0.24	26	7	2
1212+147	+75	1.621	1.45	0.30	24	6	0
1216+069	+68	0.334	0.80	0.19	53	7	1
1222+228	+82	2.046	0.84	0.24	150	8	2
1229+204	+82	0.064	0.61	0.12	118	6	2
1231+133	+75	2.386	0.74	0.32	162	14	0
1232+134	+75	2.363	2.02	0.35	98	5	0
1235+089	+71	2.885	2.29	0.29	21	4	0
1244−255	+37	0.633	8.40	0.20	110	1	4
1246−057	+57	2.222	0.91	0.28	146	9	0
1246+377	+80	1.241	1.71	0.58	152	10	2
1252+119	+75	0.870	2.51	0.56	129	6	6
1253−055	+57	0.536	9.00	0.40	67	1	4
1254+047	+67	1.024	1.22	0.15	165	3	1
1255−316	+31	1.924	2.20	1.00	153	12	4
1303+308	+85	1.770	1.12	0.56	170	14	3
1308+326	+83	0.996	12.10	1.50	68	3	4
1309−216	+41	1.491	12.30	0.90	160	2	4
1309−056	+57	2.212	0.78	0.28	179	11	0
1318+290	+83	0.549	0.61	0.28	51	13	2
1321+294	+83	0.960	1.20	0.27	111	6	2
1322+659	+51	0.168	0.81	0.22	90	8	1
1328+307	+81	0.849	1.29	0.49	47	11	3
1331−011	+60	1.867	1.88	0.31	29	5	0
1334−127	+48	0.541	10.60	0.50	8	1	4
1340+289	+79	0.905	0.81	0.35	45	12	2
1347+539	+61	0.976	1.73	0.81	161	14	6
1351+640	+52	0.087	0.66	0.10	11	4	2
1354−152	+45	1.890	1.40	0.50	46	10	4
1354+213	+74	0.300	1.42	0.31	81	6	1
1411+442	+67	0.089	0.76	0.17	61	6	1
1413+117	+65	2.542	1.53	0.31	60	6	0

Table 3. The final sample of 170 polarized quasars (continued)

Object	b_{II}	z	p	σ_p	θ	σ_θ	Ref
1416−129	+45	0.129	1.63	0.15	44	3	1
1416+067	+61	1.439	0.77	0.39	123	14	2
1425+267	+69	0.366	1.42	0.23	74	5	2
1429−008	+53	2.084	1.00	0.29	9	9	0
1435−067	+47	0.129	1.44	0.29	27	6	1
1453−109	+41	0.940	1.64	0.54	59	9	3
1458+718	+42	0.905	1.41	0.60	108	12	6
1502+106	+55	1.839	3.00	0.60	160	5	4
1504−166	+35	0.876	5.30	0.70	52	4	4
1508−055	+43	1.191	1.51	0.46	67	9	2
1510−089	+40	0.361	1.90	0.40	79	6	4
1512+370	+59	0.371	1.10	0.23	109	6	2
1522+155	+53	0.628	7.90	1.46	32	5	3
1532+016	+43	1.420	3.50	0.20	131	2	4
1538+477	+52	0.770	0.90	0.14	65	4	1
1545+210	+50	0.266	1.03	0.20	4	5	2
1548+056	+42	1.426	4.70	1.10	14	7	4
1552+085	+43	0.119	1.88	0.23	75	3	1
1611+343	+47	1.401	1.68	0.67	134	11	3
1612+266	+45	0.395	1.24	0.56	81	13	2
1617+175	+41	0.114	0.94	0.17	79	5	1
1633+382	+42	1.814	2.60	1.00	97	11	4
1635+119	+35	0.146	0.82	0.38	175	13	2
1637+574	+40	0.745	2.40	0.80	170	9	5
1641+399	+41	0.594	4.00	0.30	103	2	4
1642+690	+37	0.751	16.60	1.70	8	3	4
1656+571	+38	1.290	1.34	0.31	51	7	6
1721+343	+32	0.206	0.74	0.16	143	6	2
1739+522	+32	1.375	3.70	0.20	172	2	4
2121+050	−30	1.878	10.70	2.90	68	6	4
2131−021	−36	0.557	16.90	4.00	93	1	4
2145+067	−34	0.990	0.61	0.23	138	11	2
2154−200	−50	2.028	0.75	0.28	145	12	0
2155−152	−48	0.672	22.60	1.10	7	2	4
2216−038	−47	0.901	1.09	0.44	139	11	2
2223−052	−49	1.404	13.60	0.40	133	1	4
2225−055	−49	1.981	4.37	0.29	162	2	0
2227−088	−52	1.562	9.20	0.87	173	3	6
2230+025	−45	2.147	0.68	0.29	119	14	0
2230+114	−39	1.037	7.30	0.30	118	1	4
2240−370	−61	1.835	2.10	0.28	32	4	0
2243−123	−57	0.630	1.25	0.26	156	6	6
2245−328	−63	2.268	2.30	1.10	73	13	4
2247+140	−39	0.237	1.39	0.38	75	8	2
2251+113	−42	0.323	1.00	0.15	49	4	2
2251+158	−38	0.859	2.90	0.30	144	3	4
2251+244	−31	2.328	1.34	0.67	113	14	3
2254+024	−49	2.090	1.67	0.75	2	13	6
2255−282	−65	0.926	2.00	0.40	112	6	4
2308+098	−46	0.432	1.14	0.16	105	4	2
2326−477	−64	1.302	1.00	0.30	103	8	4
2340−036	−61	0.896	0.87	0.25	130	8	2
2345−167	−72	0.576	4.90	1.50	70	8	4
2349−010	−60	0.174	0.91	0.21	143	7	2
2351−154	−72	2.665	3.73	1.56	13	12	2
2353+283	−33	0.731	1.43	0.54	76	11	3
2354−117	−70	0.949	2.00	0.40	105	6	4
2355−534	−62	1.006	3.70	0.60	126	4	4

References: (0) Hutsemékers et al. 1998, (1) Berriman et al. 1990, (2) Stockman et al. 1984, (3) Moore & Stockman 1984, (4) Impey & Tapia 1990, (5) Impey et al. 1991, (6) Wills et al. 1992

idence for significant deviations from a uniform distribution of angles, except in the subsample of 75 quasars which are located in the southern galactic hemisphere. In this case, the Kuiper statistic is evaluated to be $K_n = 1.694$, which indicates a rejection of the null hypothesis at the 5% significance level (cf. Arsham 1988), i.e. a marginal evidence for a deviation from uniformity.

We may also test the statistical isotropy of the histograms (cf. Fig. 4) using the Hawley & Peebles (1975) Fourier method. Similar results are obtained i.e. no significant deviation from a uniform distribution of angles, except in the southern subsample. If Δ_1 and Δ_2 denotes the coefficients of the wave model which describe the degree of deviation from isotropy, we have $\Delta_1 = -0.082$ and $\Delta_2 = -0.452$ assuming the polarization angles of the 75 quasars grouped in 18 bins of 10°. Then the probability that the total amplitude $\Delta = (\Delta_1^2 + \Delta_1^2)^{1/2}$ exceeds some chosen value is computed to be $P(>\Delta) = 2\%$, using $P(>\Delta) = \exp(-0.25\, n\, \Delta^2)$ where $n = 75$ (cf. Hawley & Peebles 1975). This indicates a moderate deviation from isotropy. The preferred orientation may be calculated from $\theta = 0.5 \arctan(\Delta_2/\Delta_1) \simeq 130°$ which corresponds to the peak seen in the histogram (Fig. 4).

Taking into account the fact that we have considered several subsamples with one moderate detection, we may conclude that there is only weak evidence that the distribution of quasar polarization angles deviates from uniformity.

4.2. Maps of quasar polarization vectors

In Fig. 5, maps of quasar polarization vectors are illustrated. The whole sky is split in two parts which correspond to the northern and southern galactic hemispheres. Nearly all of the 170 quasars of our sample are represented (except 5 objects with $z > 2.3$ located in the northern galactic hemisphere). The objects are represented in redshift slices whose values have been searched for and chosen to emphasize visible alignments. The region discussed in Sect. 2 (Fig. 1) is seen in the lower left frame (with $170° \leq \alpha \leq 220°$ and $1.0 < z \leq 2.3$). In the following, we will refer to it as to the region of (quasar polarization vector) alignments A1.

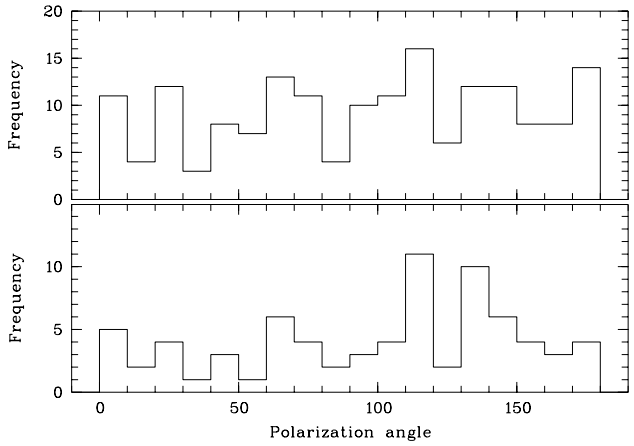

Fig. 4. Polarization angle histograms for the whole sample of 170 quasars (top), and for the 75 quasars located in the southern galactic hemisphere (bottom)

Although this may be quite subjective and dependent on the projection, at least 2 other large regions where quasar polarization vectors seem coherently oriented may be identified: a group of objects with polarization angles concentrated around $\theta \simeq 80°$ and located at roughly constant declination $\delta \sim 10°$ with $150° \leq \alpha \leq 250°$ and $0.0 < z \leq 0.5$ (region A2), and more particularly a well-defined group of 10 objects with $320° \leq \alpha \leq 360°$ and $0.7 < z \leq 1.5$, for which all polarization angles lie in the range $103° - 144°$ (region A3). The latter objects are the main contributors to the peak seen in the histogram of the southern subsample (Fig. 4). For these quasars, most measurements (i.e. 7 out of 10) are apparently taken from the same paper (Impey & Tapia 1990), giving the impression that we could have pointed out an instrumental bias. But one should recall that the paper by Impey & Tapia (1990) is also a compilation, and that 3 of these objects were in fact measured independently. Furthermore, for 2 of them (2223-052 and 2251+158) the polarization angles were re-measured by Wills et al. (1992) and are in excellent agreement, such that there is finally more evidence *against* an instrumental bias. Note that a confirmation of the reality of these alignments may simply be obtained by performing new optical polarization measurements for other quasars located in the same regions of the sky.

It is particularly interesting to notice that the alignments of quasar polarization vectors are spatially delimited, and more particularly in redshift: quasars located along the same line of sight but with lower or higher redshifts do not show the same trend. This indicates not only that a 3D analysis is essential, but also that instrumental or interstellar polarization are not likely to be responsible for the observed effect.

5. Statistical tests: formulation and description

5.1. A new dedicated statistical test

Apart from the fact that the identified polarization vector alignments are apparently localized in the 3D space, we have a priori no idea on their characteristics, nor on the physics responsible for them. Statistical tests should therefore be general enough, and if possible non-parametric, the main goal being the detection of the effect and the evaluation of its statistical significance. For this purpose, we design a rather simple measure of polarization vector alignments, which will be compared to simulations.

First, we adopt comoving distances calculated with

$$r(z) = \frac{2\,c}{H_0}\,(1 - (1+z)^{-1/2})\,, \tag{1}$$

where we assume a flat Universe with a cosmological deceleration parameter $q_0 = 0.5$. H_0 is the Hubble constant; its value is unimportant here since only relative distances are of interest. The distance from an object to another one is then computed using the rectangular coordinates

$$\begin{aligned} x &= r\,\cos\delta\cos\alpha\,,\\ y &= r\,\cos\delta\sin\alpha\,,\\ z &= r\,\sin\delta\,, \end{aligned} \tag{2}$$

α and δ denoting the right ascension and declination of the object in the equatorial coordinate system. A 2D analysis may be carried out by fixing $r = 1$ in Eq. 2.

For each group of n_v neighbouring quasars, we consider the local dispersion of polarization angles as a measure of their possible alignment. For evaluating a circular dispersion, there are several possibilities which are essentially related to the *mean* direction of the angles, or to the *median* direction (cf. Fisher 1993). After some experimentation, the dispersion related to the median was adopted, since it appeared slightly more efficient in detecting local deviations from uniform distributions of angles. For each object, we identify the n_v nearest neighbours in the 3D (or 2D) space, and compute (Fisher 1993)

$$d(\theta) = 90 - (1/n_v)\sum_{k=1}^{n_v} |90 - |\theta_k - \theta||, \tag{3}$$

where $\theta_1, \cdots, \theta_{n_v}$ are the polarization angles of the neighbouring objects. The central object is included in the n_v ones and in the sum (with $k = 1$). In this expression, it has been accounted for the fact that polarization angles are *axial* data, i.e. they do not span the whole circle but range from 0° to 180°. The mean dispersion of the polarization angles of the n_v objects around object i, hereafter noted D_i, is computed to be the minimum value of $d(\theta)$. If n represents the total number of objects in our sample, we adopt

$$S_D = \frac{1}{n}\,\sum_{i=1}^{n} D_i \tag{4}$$

as a statistic with one parameter n_v. If the polarization vectors are locally aligned, we expect S_D to be smaller than in models where polarization angles are distributed at random on the objects.

S_D measures the concentration of angles for groups of objects close to each other in space. We may also measure, in a

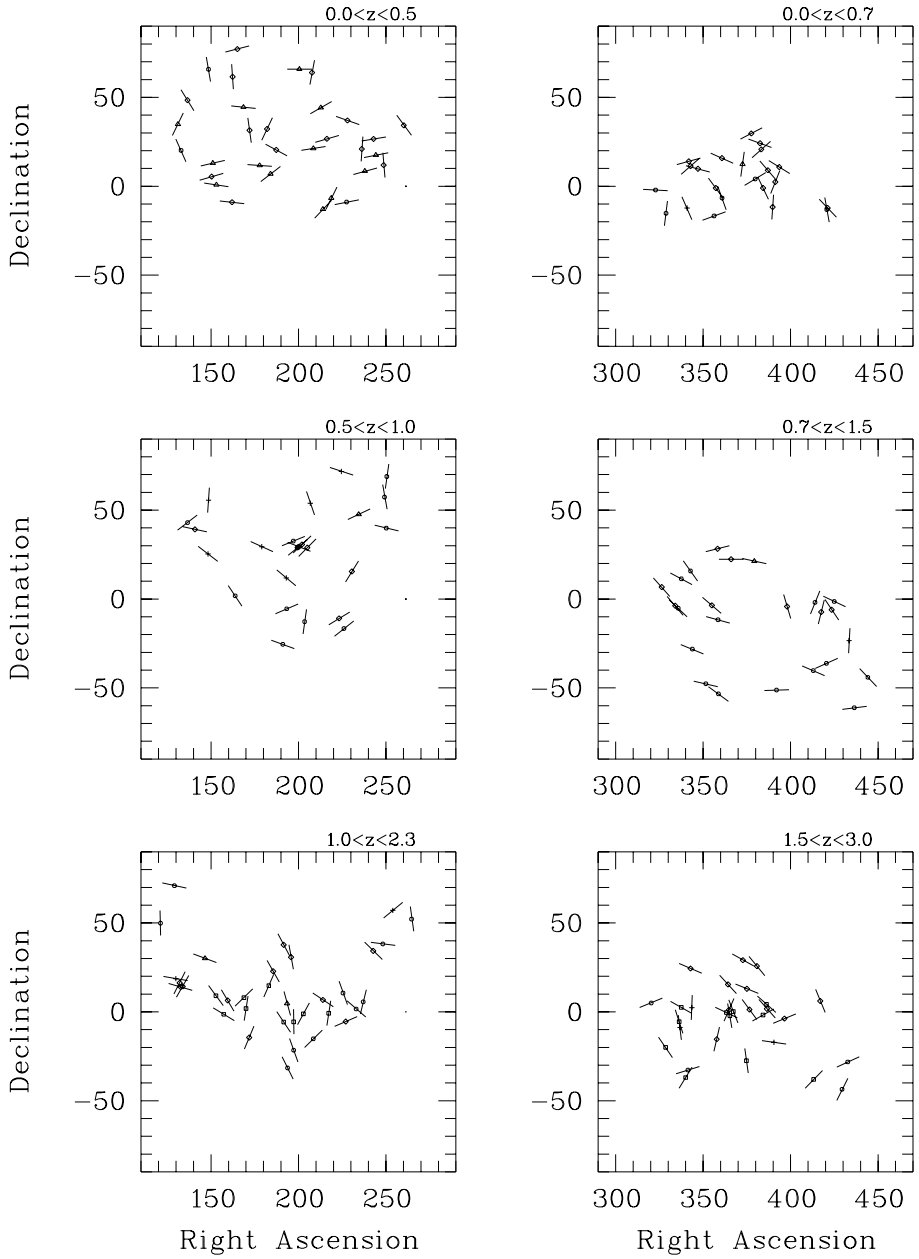

Fig. 5. Maps of quasar polarization vectors in the equatorial coordinate system (right ascensions are in degrees). Each frame is labeled with the redshift range. The different symbols refer to different catalogues: Stockman et al. 1984, and Moore & Stockman 1984 [losanges], Berriman et al. 1990 [triangles], Impey & Tapia 1990, and Impey et al. 1991 [circles], Wills et al. 1992 [crosses], Hutsemékers et al. 1998 [squares]

given volume, the spatial concentration of objects which have similar angles. The combination of both measures is expected to be more efficient for detecting local coherent orientations, for example if groups of aligned neighbours have different sizes, or if their shape is not spherical.

So, for each object i, we first compute an average direction of the polarization angles of its n_v nearest neighbours, including the object i itself. The average direction is taken to be the median direction $\tilde{\theta}$ which is the value of θ minimizing the function $d(\theta)$ in Eq. 3. The median is not always uniquely defined since $d(\theta)$ may not have a single minimun, or this minimum may be quite broad: this situation occurs when the angles tend to be uniformly distributed, and more particularly when n_v is small. In this case, we choose for the median direction the central value of the broadest minimum, taking into account the circular nature of the data. Note that other kinds of average directions may be considered, like the mean direction defined in the next section (Eq. 11) which provides comparable results.

To every object k taken among the n_v neighbours and whose polarization angle θ_k is close to the local median, i.e. objects for which $\Delta\theta_k \leq \Delta\theta_c$ where

$$\Delta\theta_k = 90 - |90 - |\theta_k - \tilde{\theta}|| \tag{5}$$

and $\Delta\theta_c$ is a critical value defined between 0° and 90° and fixed in advance, we attribute a weight w_k = 1, otherwise w_k = 0. Then, if $r(k, k')$ represents the distance from object k to

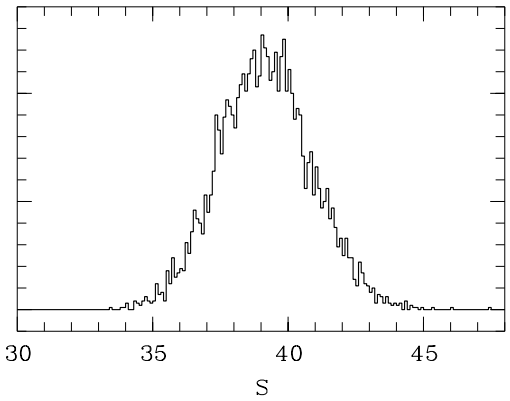

Fig. 6. An example of the S distribution obtained by running 5000 simulations, with n_v = 24 and $\Delta\theta_c$ = 60°. With the same parameters, the S statistic corresponding to our sample of 170 quasars is computed to be $S^\star$ = 33.°9

object k', we calculate the average distances

$$RC_i = \frac{\sum_{k=1}^{n_v-1}\sum_{k'=k+1}^{n_v} w_k w_{k'}\, r(k,k')}{\sum_{k=1}^{n_v-1}\sum_{k'=k+1}^{n_v} w_k w_{k'}}\,, \tag{6}$$

which refers to objects whose polarization angles are close to the median direction, and

$$RF_i = \frac{\sum_{k=1}^{n_v-1}\sum_{k'=k+1}^{n_v}(1-w_k)(1-w_{k'})\, r(k,k')}{\sum_{k=1}^{n_v-1}\sum_{k'=k+1}^{n_v}(1-w_k)(1-w_{k'})}\,, \tag{7}$$

which refers to objects whose polarization angles are far from the median direction, the ratio

$$R_i = RC_i/RF_i \tag{8}$$

providing a local measure of the spatial concentration of objects which have angles close to the median. R_i is expected to be around 1 when the angles are distributed at random on the different objects, and smaller than 1 when objects with similar angles are spatially concentrated. Its value is put equal to 1 when the number of objects with w_k = 1 or the number of objects with w_k = 0 is strictly smaller than 3.

We can now write the final statistic

$$S = \frac{1}{n}\sum_{i=1}^{n} D_i\, R_i\,, \tag{9}$$

which may be evaluated for different values of the parameters n_v and $\Delta\theta_c$. It is expected to be relatively small for samples in which local alignments of polarization vectors are present.

Since the quantities D_i and R_i are clearly not independent due to the overlapping regions over which they are calculated, the distribution of S and S_D must be obtained using simulations. For this, the positions of the objects are kept fixed, and the polarization angles randomly shuffled on the objects. With this method, each simulated configuration has the same angle histogram and object positions as the original sample, but any true correlation between angles and positions will have been erased, ensuring that we are essentially testing correlations between angle coherent orientations and object positions. Several thousand simulated configurations are computed for which the S and S_D statistics are evaluated. A typical example of the S distribution is illustrated in Fig. 6, for n_v = 24 and $\Delta\theta_c$ = 60°. With different values of the parameters, the distribution is shifted or its shape modified.

If $S^\star$ is the statistic measured for the original sample, the statistical significance of the test, or the probability that a value of S such that $S < S^\star$ would have been obtained by chance, may be estimated in computing the percentage of simulated configurations for which $S < S^\star$, up to a resolution fixed by the number of simulations.

Let us finally note that distributions resulting from randomly generated (instead of shuffled) angles have also been tried, and that they give nearly similar statistical significances.

5.2. The Andrews & Wasserman test

After the previously described test was implemented, and most results obtained, we became aware of the work by Bietenholz & Kronberg (1984), and Bietenholz (1986). These authors have re-analysed with appropriate statistical methods the claim by Birch (1982) that the offset between the position angle of an extragalactic radio source and the orientation of its radio polarization vector (corrected for Faraday rotation) is correlated with the source position on the celestial sphere. Although the results themselves may be of interest for the present study and will be discussed later, we consider here one of the proposed statistical tests which may be useful for our purpose: the non-parametric test originally due to Andrews & Wasserman.

The idea of the Andrews & Wasserman test is to compute for each object i, the mean direction $\bar\theta_i$ of its n_v neighbours, and to compare this local average to the actual polarization angle of the object i, θ_i. If angles are correlated to positions, one expects, on the average, θ_i to be closer to $\bar\theta_{j=i}$ than to $\bar\theta_{j\neq i}$.

So, for each object i, we consider the n_v nearest neighbours in the 2D or 3D space as in Sect. 5.1, and compute the mean resultant vector

$$\mathbf{Y}_i = \frac{1}{n_v}\,(\sum_{k=1}^{n_v}\cos 2\theta_k,\ \sum_{k=1}^{n_v}\sin 2\theta_k)\,, \tag{10}$$

where $\theta_1, \cdots, \theta_{n_v}$ are the polarization angles of the neighbouring objects, excluding i. The factor 2 accounts for the fact that the polarization angles are axial data. Then, if we let $\bar{\mathbf{Y}}_i$ denote the normalized vector $\mathbf{Y}_i$, the mean direction $\bar\theta_i$ is given by

$$\bar{\mathbf{Y}}_i = (\cos 2\bar\theta_i,\ \sin 2\bar\theta_i)\,. \tag{11}$$

As a measure of the closeness of θ_i and $\bar\theta_j$, one uses the inner (dot) product $\mathrm{D}_{i,j} = \mathbf{y}_i.\bar{\mathbf{Y}}_j$, where $\mathbf{y}_i = (\cos 2\theta_i, \sin 2\theta_i)$. If angles are correlated to positions, $\mathrm{D}_{i,j}$ is expected to be, on the average, larger for $j = i$ than for $j \neq i$. Then, to evaluate the statistic, one sorts the $\mathrm{D}_{i,j=1,n}$ values in increasing order, and notes r_i the rank of $\mathrm{D}_{i,j=i}$. Finally, the test statistic Z_c, which

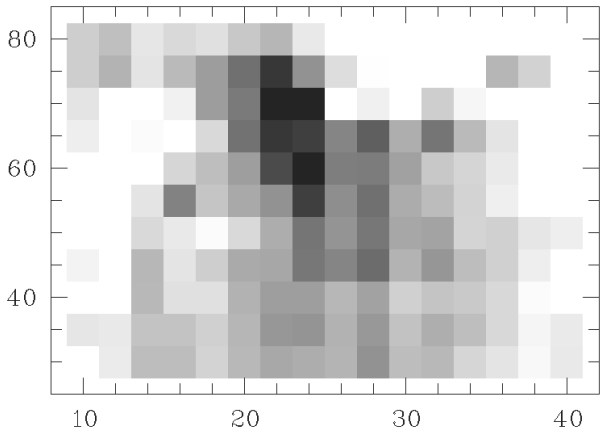

Fig. 7. Map of the significance level of the S statistical test applied to our sample of 170 quasars for various combinations of the parameters n_v (in abscissae) and $\Delta\theta_c$ (in ordinates). The significance level is represented on a logarithmic gray scale where white corresponds to log S.L.≥ -1.3 and black to log S.L.≤ -3

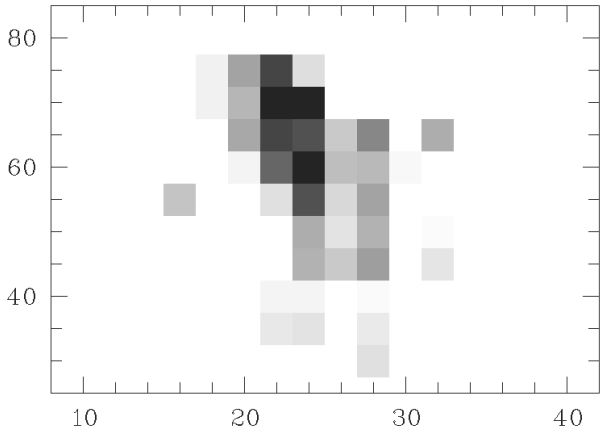

Fig. 8. Same as Fig. 7, but white corresponds to log S.L.≥ -2 and black to log S.L.≤ -3. The smallest value of the S.L. is $2\,10^{-4}$, for n_v = 22 and $\Delta\theta_c$ = 70°

is approximately normally distributed (cf. Bietenholz 1986), is written

$$Z_c = \frac{1}{n} \sum_{i=1}^{n} Z_i \tag{12}$$

where

$$Z_i = \frac{\mathrm{r}_i - (n+1)/2}{\sqrt{n/12}}\,, \tag{13}$$

n representing the total number of objects in our sample. Z_c is expected to be significantly larger than zero when the polarization angles are not randomly distributed on object positions. Again, the number of nearest neighbours n_v is a free parameter.

Although this test is normalized, the $\mathrm{D}_{i,j=1,n}$ are not independent, especially for large n_v. When applied to our sample, simulations were found necessary to obtain accurate statistical

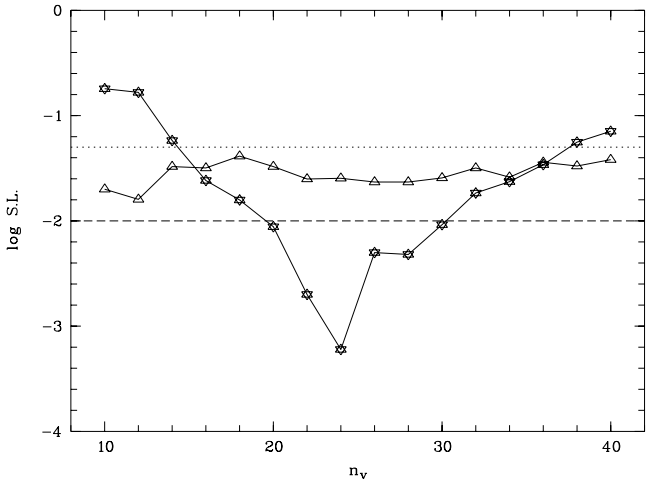

Fig. 9. The significance level of the S_D test (triangles) as a function of n_v for our sample of 170 quasars, together with the results of the S test for $\Delta\theta_c$ = 60° (stars). The dotted and dashed horizontal lines respectively indicate S.L. = 0.05 and 0.01

significances, i.e. to better than a factor 2-3. If $Z_c^\star$ is the statistic measured for the original sample, the statistical significance of the test may be evaluated by computing the percentage of simulated configurations for which $Z_c > Z_c^\star$.

5.3. A modified Andrews & Wasserman test

The original Andrews & Wasserman test may be modified in an interesting way. The length of the mean resultant vector $\mathbf{Y}_i$ provides in fact a natural measure of the dispersion of the angles, being large if the angles are concentrated around the mean direction (e.g. Fisher 1993). By using the dot product $\mathrm{D}_{i,j} = \mathbf{y}_i.\mathbf{Y}_j$ instead of $\mathrm{D}_{i,j} = \mathbf{y}_i.\bar{\mathbf{Y}}_j$, one gives more weight to the groups of objects for which the local average has actually a sense, i.e. to those for which the polarization vectors are coherently oriented. Apart from this, the statistic Z_c^m of this modified Andrews & Wasserman test is calculated in the same way.

5.4. Visualization of the results

The previous tests may tell us if a statistically significant orientation effect exists in the sample, or not. However, it would be interesting to know which groups of objects contribute the most to the effect, and if the groups visually identified in Fig. 5 have some statistical reality or not. For this, we use a method adapted from Dressler & Shectman (1988) which was proposed for detecting sub-structures in clusters of galaxies.

For each object i, a local statistic S_i has been defined: S_i = D_i, D_iR_i, Z_i or Z_i^m (cf. Eqs. 4, 9, 12). It may be evaluated for the original sample, $S_i^\star$, as well as for every simulated configuration, such that one can compute $< S_i >$, the average over the whole set of simulations, and σ_i, the corresponding standard deviation. Then we calculate

$$s_i = \frac{< S_i > - S_i^\star}{2\,\sigma_i}\,, \tag{14}$$

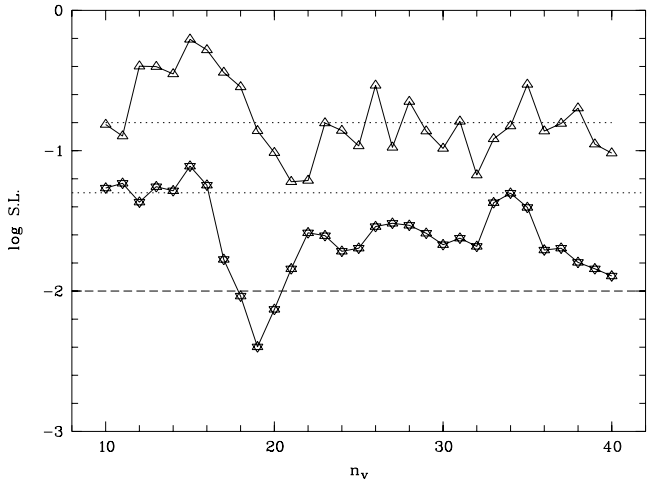

Fig. 10. The significance level of the Z_c and Z_c^m tests (respectively, triangles and stars) as a function of n_v for our sample of 170 quasars. For clarity, the Z_c results have been shifted upwards by 0.5. The dotted and dashed horizontal lines respectively indicate S.L. = 0.05 and 0.01

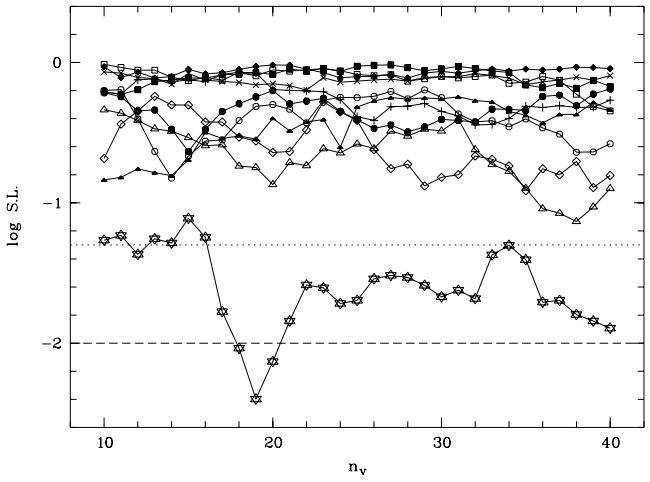

Fig. 12. The significance level of the Z_c^m test as a function of n_v for our sample of 170 quasars, when the test is applied to the real data (stars), and to the first ten randomized models (other symbols). The dotted and dashed horizontal lines respectively indicate S.L. = 0.05 and 0.01

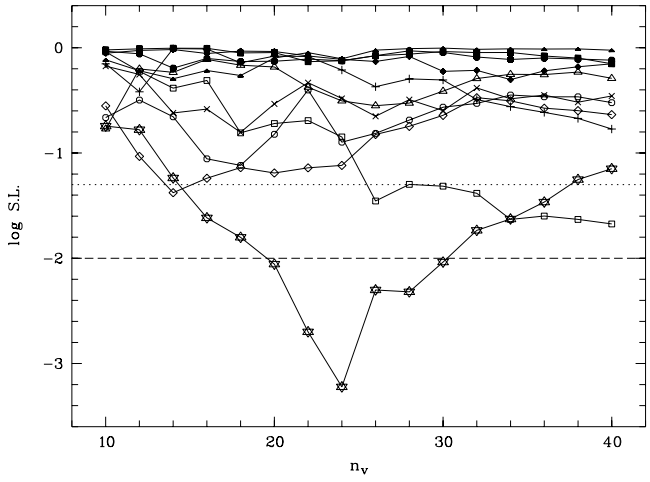

Fig. 11. The significance level of the S test ($\Delta\theta_c = 60^\circ$) as a function of n_v for our sample of 170 quasars, when the test is applied to the real data (stars), and to the first ten randomized models (other symbols). The dotted and dashed horizontal lines respectively indicate S.L. = 0.05 and 0.01

which provides a measure of the local departure to random models. If we only consider the positive values of s_i when $S_i = D_i$ or $S_i = D_i R_i$, and the negative values of s_i when $S_i = Z_i$ or $S_i = Z_i^m$, one may draw around each object i a circle of radius

$$\rho_i \propto \exp|s_i| - 1\,, \tag{15}$$

such that the larger the circle, the larger the contribution of object i to a local orientation effect. Put on maps, clusters of large circles may help to identify regions in which polarization vector alignments prevail, if one carefully keeps in mind that the points are not statistically independent.

6. Results from the statistical tests

The selected sample of 170 quasars has been analysed using the tests S, S_D, Z_c, and Z_c^m, and considering the objects located in the 3D space. The parameters have been varied around values expected from the preliminary analyses (Sects. 2 & 4), then largely explored to check the behavior and stability of the results. Finally, the test statistics have been computed for n_v between 10 and 40 nearest neighbours, and $\Delta\theta_c$ between 30° and 80°. Let us recall that n_v represents the number of neighbours including the central object for the S-type tests, while excluding it for the Z-type tests. As far as computing time is concerned, the Z-type tests are significantly faster than the S-type ones such that smaller increments in n_v were taken to allow a direct comparison of the results. In order to evaluate the significance level of the statistical tests, 5000 models with randomly shuffled angles have been considered. The tests were applied to each randomized model for the adopted range of parameters, and statistical distributions have been constructed for each n_v, or combination of n_v and $\Delta\theta_c$. The test statistics computed for the real data with a given set of parameters were then compared to the statistical distributions obtained with the same parameters.

The results of the S test, which depend on both n_v and $\Delta\theta_c$, are conveniently illustrated in Figs. 7 & 8, which represent maps of the significance level (S.L.) in the (n_v, $\Delta\theta_c$)-plane. Only S.L. evaluated to be lower than 0.05 (0.01) are illustrated in Fig. 7 (Fig. 8), the darker the points the smaller the S.L. We emphasize that the S.L. values are not independent. The variation with the parameters appears rather smooth, and a significant deviation from randomness is detected around $n_v \sim 24$ with $0.001 <$ S.L. < 0.01, quite independently of $\Delta\theta_c$ (Fig. 8). Significance levels as small as $2\,10^{-4}$ were measured but are not considered as representative. The values of n_v which minimize the S.L., although larger than the 10-15 coherently oriented objects

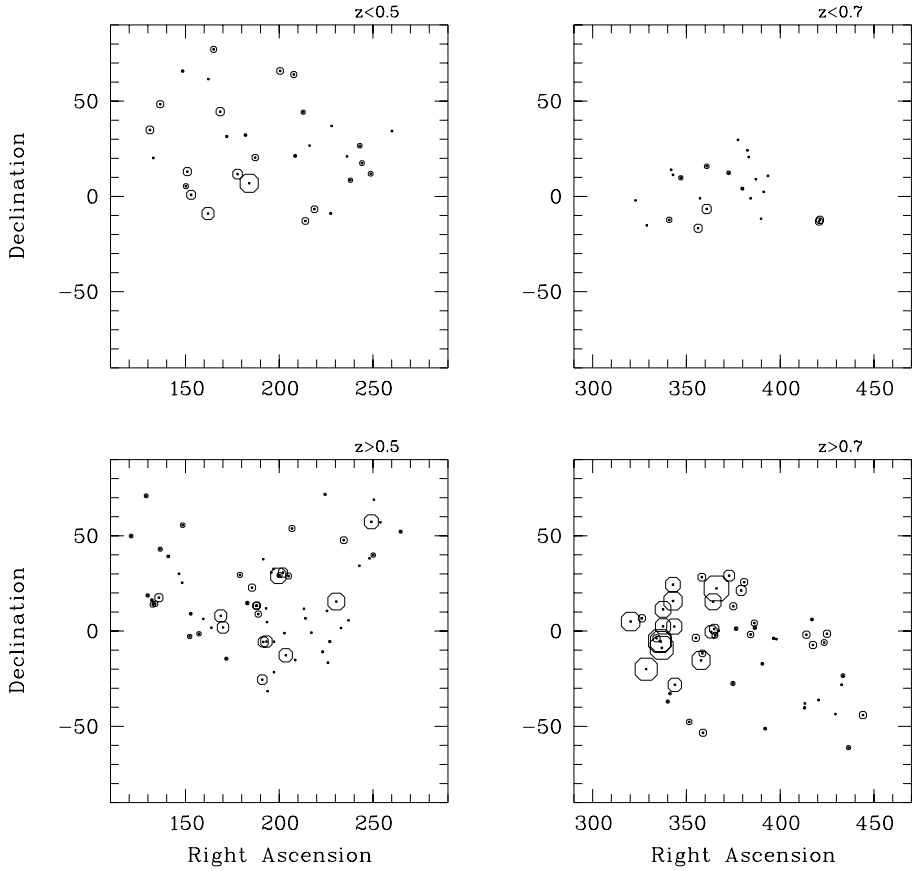

Fig. 13. Maps in the equatorial coordinate system of the local contributions to the significance level of the S test, for n_v = 24 and $\Delta\theta_c$ = 60°. Each frame is labeled with the redshift range

visually identified in Fig. 5, are in good agreement with the expected values since the number of neighbours used in the tests must necessarily encompass the physical structures, due to the way the tests are designed. In addition, these structures may be slanted with respect to the line of sight and contain more members than actually seen on projected maps.

The results of the S_D test, which do not depend on $\Delta\theta_c$, are given in Fig. 9 together with a representative example of the S test obtained for $\Delta\theta_c$ = 60°. As expected, the S_D test is less sensitive, although it indicates moderate deviation from randomness with $0.01 <$ S.L. < 0.05, quite independently of n_v. The S.L. of the Z-type tests are illustrated in Fig. 10. The Z_c^m test detects a deviation from uniformity for $n_v \simeq 18 - 20$ with S.L. < 0.01, confirming the previous results. The Z_c test appears to be the less sensitive with a rather noisy S.L. It nevertheless indicates a moderate deviation from randomness near $n_v \sim 22$ with $0.01 <$ S.L. < 0.05. The slightly larger values of n_v obtained with the S test when compared to the Z_c^m test may probably be accounted for by the fact that one needs at least three mis-aligned objects among the n_v nearest neighbours for computing the distance ratio R_i (Eq. 8).

Although there is a good agreement between the values of n_v minimizing the significance level of the statistical tests and those expected from Fig. 5 (the results are not too dependent on $\Delta\theta_c$), the parameter values were in fact not exactly known a priori. It is therefore important to have an estimate of the significance independently of the values of $\Delta\theta_c$ and n_v. Since the results at different $\Delta\theta_c$ and n_v are not independent, we have computed for each of the 5000 randomized models the smallest S.L. given by the tests for whatever n_v and $\Delta\theta_c$ it occurs at, and constructed the distribution of these minimum values. Since the minimum S.L. does not occur at the same n_v or $\Delta\theta_c$ for the different realizations (cf. Figs. 11 & 12), S.L. have been used instead of statistics, the latter being not normalized. Then, the smallest S.L. for the real data, also evaluated whatever the value of n_v or $\Delta\theta_c$, has been compared to the previously obtained distribution, and a "global" S.L. derived. Considering the whole range of $\Delta\theta_c$ and n_v, i.e. $\Delta\theta_c$ = 30° to 80° and n_v = 10 to 40, the global S.L. is found to be equal to 0.005 for the S test. For the Z_c^m test, the global S.L. is 0.015 with n_v = 10 to 40. Since the parameter space has been more largely explored than necessary, these values may be seen as upper limits.

Now, it is interesting to see which groups of objects contribute the most to the deviation, and if they correspond, or not, to the regions of alignments visually identified in Sect. 4.2. The local contributions to the significance levels of the S and Z_c^m tests are illustrated for a representative case in Figs. 13 & 14 where the 170 quasars are plotted on maps comparable to those of Fig. 5, following the method described in Sect. 5.4. Note that we should not expect a one-to-one correlation between the quasars whose polarization vectors are apparently aligned and those associated with a small local significance level. On the

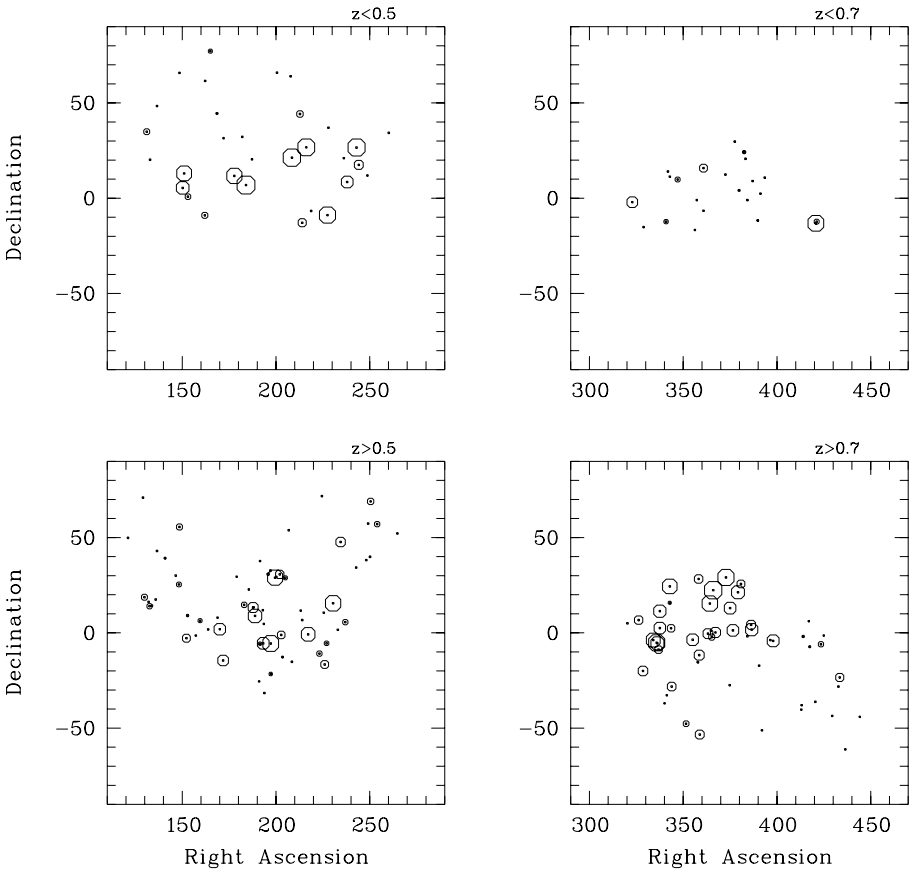

Fig. 14. Maps in the equatorial coordinate system of the local contributions to the significance level of the Z_c^m test, for n_v = 19. Each frame is labeled with the redshift range

maps, the larger and more numerous the circles, the larger the contribution to a local deviation from uniformity, although we re-emphasize that large circles are not independent. It can be seen from Figs. 13 & 14 that the strongest concentration of large circles roughly coincides with the high redshift region of alignments A3 ($320^\circ \leq \alpha \leq 360^\circ$; cf. Fig. 5 and Sect. 4.2). Nearby and also contributing is a small group of quasars located at $\alpha \sim 10^\circ$, $\delta \sim 20^\circ$, which may be identified on the high redshift ($z \geq 1.5$) map of Fig. 5; it could constitute an extension of region A3. Large regions with little or no circles are also seen: the contrast between the high and low redshift maps is particularly striking. This statistically confirms that the regions of polarization vector alignments are spatially delimited, namely in redshift. Significant local deviations from randomness also coincides with the high redshift region A1 ($170^\circ \leq \alpha \leq 220^\circ$), suggesting it is detected by the tests, although not as strongly as region A3. This difference may be due to the fact that the most aligned objects of region A1 lie in a relatively narrow region (cf. Sect. 2), while the tests are more efficient for detecting spherical structures. This nevertheless confirms the preliminary detection of region A1 reported in Sect. 2. Finally, the low redshift region A2 is also possibly detected, but mainly by the Z_c^m test. Note that similar conclusions are reached when considering other combinations of $\Delta\theta_c$ and n_v associated with small S.L. These results indicate that the statistically significant groups of objects are spatially delimited, namely in redshift, and that they correspond reasonably well to the regions visually identified in Fig. 5.

Finally, the statistical tests were run in 2D assuming all quasars located at the same distance, i.e. on the surface of a sphere (r = 1 in Eq. 2). The significance levels are definitely worse than in the 3D case. Typical results are illustrated in Fig. 15: for all n_v, S.L. > 0.01 with the S test, and S.L. > 0.05 with the Z_c^m test. This suggests weak to no real evidence for deviations from uniformity when the 3D positions of the objects are not fully taken into account.

6.1. The importance of the selection criteria

Our sample of 170 quasars was obtained by applying quite severe selection criteria to eliminate at best the contamination by our Galaxy (cf. Sect. 3). In order to know a posteriori if these were justified, we completely relax the constraints on b_{II} and p before applying the tests again. Although the size of the sample increases to 249 quasars, none of the S or Z-type tests indicate significant deviations from randomness, suggesting that the contamination is real when no selection is applied, in agreement with the study by Berriman et al. (1990, cf. Sect. 3). On the contrary, if the constraints are too strong, the sample is too small and significant results cannot be obtained. It is nevertheless interesting to note that with the condition $|b_{II}| \geq 35^\circ$ instead of $|b_{II}| \geq 30^\circ$, a deviation from uniformity is detected by both the

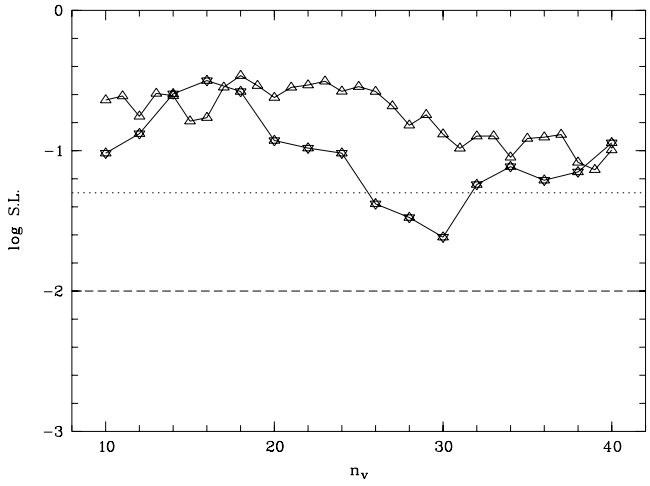

Fig. 15. The significance level of the Z_c^m and S tests (respectively, triangles and stars) as a function of n_v for our sample of 170 quasars, when all quasars are assumed located at the same distance (2D case). For the S test, $\Delta\theta_c$ = 60°. The dotted and dashed horizontal lines respectively indicate S.L. = 0.05 and 0.01

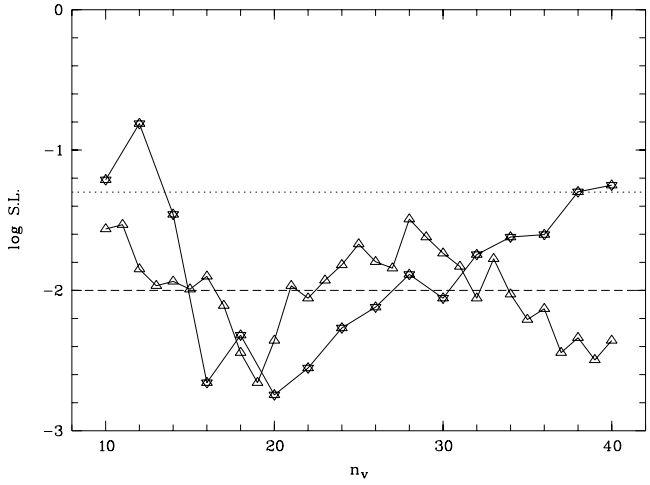

Fig. 16. The significance level of the Z_c^m and S tests (respectively, triangles and stars) as a function of n_v for a more constrained sample of 153 quasars. For the S test, $\Delta\theta_c$ = 60°. The dotted and dashed horizontal lines respectively indicate S.L. = 0.05 and 0.01

S and Z_c^m tests with a comparable to better S.L. (cf. Fig. 16), although the size of the sample has decreased to 153 objects.

6.2. The dependence on the coordinate system

The statistical tests used in the present paper are invariant under rotations of the polarization angles and of the coordinates of the sources α and δ. In fact, since only relative distances are of interest, the object position may be expressed in any coordinate system on the celestial sphere. But this is not true for the polarization angles which are defined relative to the meridians and depend on the polar axis. The importance for the statistical tests may be easily understood if one imagines a group of objects in the sky with aligned polarization vectors: if projected on the equatorial region of the celestial sphere, the alignment will be more or less conserved and detected by the tests. However, if one puts a pole just in the middle of the group, the projected angles will range from 0° to 180° and the alignment be undetected, although the dependence of the angles on positions is still highly organized. We therefore expect the significance level of our statistical tests to vary with the adopted polar axis.

To investigate this effect, we consider a new arbitrary northern pole, the equatorial coordinates of which are α_p, δ_p. In the associated new system of coordinates, the polarization angle θ_N of an object is given by

$$\tan(\theta - \theta_N) = \frac{\cos\delta_p \, \sin\left(\alpha_p - \alpha\right)}{\sin\delta_p \, \cos\delta - \sin\delta \, \cos\delta_p \, \cos\left(\alpha_p - \alpha\right)}, \quad (16)$$

where θ is the polarization angle in the equatorial coordinate system, and α, δ the equatorial coordinates of the object. For example, polarization angles projected in galactic coordinates are computed with α_p = 192° and δ_p = 27°, which are the equatorial coordinates of the North Galactic Pole. Since the polarization vectors are not oriented, only the polar direction is meaningful, and $(\alpha_p + 180°, \delta_p)$ is equivalent to $(\alpha_p, -\delta_p)$.

For each pole (α_p, δ_p) we have therefore a different set of polarization angles for which the statistics and the significance levels may be computed. The results are illustrated in Fig. 17 which represents a map in the (α_p, δ_p)-plane of the statistic Z_c^m applied to our sample of 170 quasars and averaged over n_v = 17 to 23. Ideally one should have used S.L. instead of the statistic but at the cost of a too large amount of computing time. However, since the Z_c^m statistic is normalized, its values may be roughly seen as usual σ values, which is sufficient for the present purpose.

It is clear from Fig. 17 that the S.L. of the test depends on the adopted pole. Regions of higher and lower S.L. are clearly seen when compared to our previous results obtained in equatorial coordinates (δ_p = 90°); a spot of higher significance is identified near (130°, 35°). A very similar pattern with a spot near (120°, 35°) is observed using the S statistic suitably averaged over n_v and $\Delta\theta_c$, although this map appears less contrasted. For confirmation, the tests were run adopting the pole (125°, 35°), and the significance levels were computed. For all the S, S_D, Z_c, and Z_c^m tests, definitely lower S.L. are obtained over larger n_v ranges, S.L $< 10^{-3}$ being frequently observed. Typical examples, which should be compared to those in Fig. 10, are illustrated in Fig. 18; they were obtained by running 10000 simulations for the Z-type tests. Moreover, by visualizing the local S.L. as in Figs. 13 & 14, we have noticed that the increased significance of the tests is essentially due to the same groups of objects rather than to additional ones. Now, since the position of the spot does not correspond to the pole of an already known cosmical direction, like the Local Supercluster Pole (283°, 16°), the Cosmic Microwave Background Dipole (168°, −7°), or the direction to the Great Attractor (200°, −40°) (Bennett et al. 1996, Scaramella et al. 1989), it should not be considered as more than

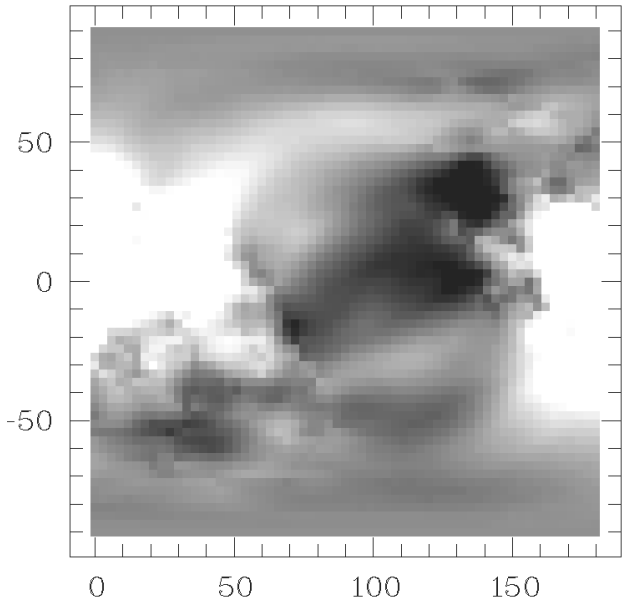

Fig. 17. Map of the Z_c^m statistic averaged over n_v = 17 to 23, as a function of the equatorial coordinates α_p (abscissae) and δ_p (ordinates) of an arbitrary northern pole. The statistic is represented on a logarithmic gray scale where white corresponds to $\overline{Z_c^m} \leq 1$ and black to $\overline{Z_c^m} \geq 3$. Note that $(\alpha_p + 180^\circ, \delta_p)$ is equivalent to $(\alpha_p, -\delta_p)$

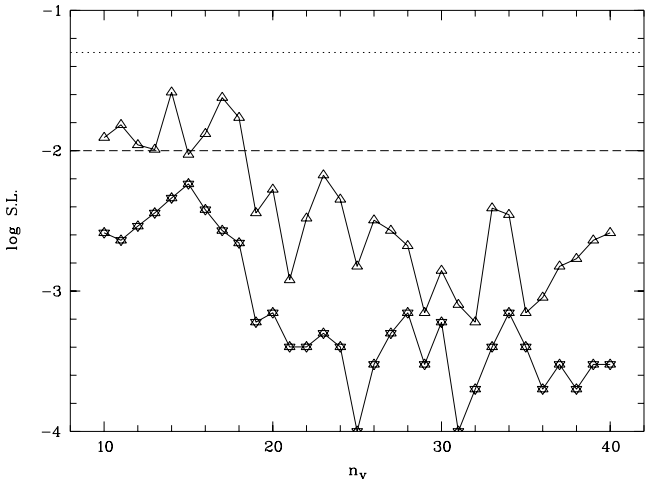

Fig. 18. The significance level of the Z_c and Z_c^m tests (respectively, triangles and stars) as a function of n_v for our sample of 170 quasars, with the polarization angles projected in a coordinate system of northern pole (α_p = 125°, δ_p = 35°). Note that for n_v = 25, the S.L. of the Z_c^m test is in fact unresolved, and therefore smaller than illustrated. The dotted and dashed horizontal lines respectively indicate S.L. = 0.05 and 0.01

a statistical fluctuation, probably due to the non-uniform distribution of coherently oriented objects in a rather limited sample. The important conclusion is that the significance of our previous results in equatorial coordinates appears intermediate and not exceptional.

6.3. Conclusions on test results

From the previous results, we may conclude that in our sample of 170 quasars, 3D statistical tests provide evidence that local alignments of polarization vectors are present, and that these cannot be ascribed to random fluctuations with global significance levels of 0.005 and 0.015, depending on the test. The higher significance reached in several cases cannot be considered as representative, but indicates that the reported significance levels are stable and not exceptional.

The tests show that the polarization vectors are coherently oriented in groups of $n_v \sim 20$ quasars, spatially delimited, and roughly corresponding to the regions visually identified on polarization vector maps. Large regions where angle distributions are compatible with random fluctuations are also seen.

7. Discussion

7.1. Are the alignments due to instrumental or interstellar polarization?

A first possible explanation for the observed polarization vector alignments is a strong instrumental bias which affects the measurements, at least for the quasars which participate to the effect. However this interpretation is unlikely since the objects with aligned polarization vectors were not measured by the same authors, nor using identical techniques (cf. Fig. 5, Sect. 4.2, and Tables 1, 2 and 3,). Also, objects measured in different surveys have polarization angles which are generally in good agreement. Furthermore, very large polarization degrees ($\geq$ 10%) are sometimes recorded and these cannot be easily ascribed to an instrumental effect. Finally, if instrumental polarization is responsible for the effect, one would expect the mean directions of the aligned polarization vectors to coincide with 0° or 90°, which is not the case.

Extinction by dust grains in our Galaxy is well known to polarize light from distant stars and to be at the origin of local alignments of polarization vectors (Mathewson & Ford 1970, Axon & Ellis 1976). Since this interstellar polarization certainly affects to some extent the quasar measurements, we have applied severe selection criteria to eliminate at best this contamination. As a whole, our final sample of 170 objects is most probably quite free of contamination, but a few affected objects may remain, and we cannot be sure a priori that these objects are not precisely those which participate to an alignment. The following discussion will therefore essentially concern the quasars belonging to the regions of alignments A1, A2 and A3, plus a few objects possibly connected to region A3 (cf. Sect. 6), i.e. a total of 43 objects.

First, if extinction in our Galaxy is the dominant mechanism of alignment, we would expect quasars located approximately along the same line of sight to have similar polarization angles independently of their redshift. The contrary is definitely observed (Fig. 5): alignments are well delimited in redshift (cf. region A3), with even different mean directions along the same

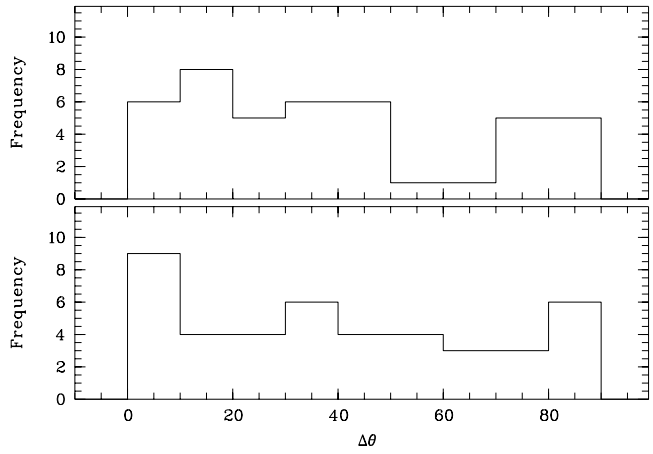

Fig. 19. Histograms of the polarization angle difference $\Delta\theta = 90 - |90 - |\theta - \theta_{star}||$, where θ refers to a quasar with aligned polarization vector and θ_{star} to the nearest galactic star on the celestial sphere. The stellar data are from the Axon & Ellis (1976) catalogue. Top: all stars are taken into account; bottom: only those stars with $d \geq 400$ pc are considered

line of sight (cf. regions A1 & A2). One might argue that the polarization degree might depend on redshift since it refers to different rest-frame spectral regions; in this case the quasar polarization could be significantly smaller for some redshift ranges and the contamination by the Galaxy larger. But, on the average, p is not smaller for quasars with aligned polarization vectors than for objects at lower or higher redshifts located along the same line of sight (cf. Tables 1, 2 and 3); moreover some of these quasars have very large p values which are difficult to ascribe to interstellar polarization, especially at high galactic latitudes. For comparison, if we consider distant stars located at high galactic latitudes (i.e. 150 stars with $d \geq 400$pc and $|b_{II}| \geq 30°$ from the catalogue of Axon & Ellis 1976), only 10 of them have $p \geq 0.6\%$ and 2 have $p \geq 1.0\%$ (cf. Fig. 2). Low polarizations ($p \leq 0.3\%$) are also reported by Berdyugin & Teerikorpi (1997) for stars close to the North Galactic Pole. In fact, the polarization degree of quasars with aligned polarization vectors is significantly higher than that of galactic stars located nearby on the celestial sphere, which is a direct consequence of our selection criteria. In addition, these quasars are not located in regions of particularly high extinction: when reported on the Burstein & Heiles (1982) extinction maps, nearly all objects are located in regions where interstellar $E_{B-V} \leq 0.03$, i.e. $p_{ISM} \leq 0.3\%$. In fact, the existence of a correlation between quasar structural axis and polarization angle indicates that the polarization is essentially intrinsic to the objects (Rusk 1990, Impey et al. 1991). This also means that the Galaxy should first de-polarize the light before producing alignments, such that even more obscuring material would be needed for affecting quasars than for affecting distant unpolarized stars.

Now, in order to compare the polarization angles themselves, we have searched in the Axon & Ellis (1976) catalogue the nearest polarized galactic star to each quasar which participates to an alignment. As seen in Fig. 19, no relation is found between the angles, i.e. no major concentration near $\Delta\theta \sim 0°$ in the histograms. Similar results are obtained when considering more than one nearest star. The three groups of aligned polarization vectors have also been compared to the global orientations seen throughout the Galaxy, namely on the maps of Axon & Ellis (1976) and Mathewson & Ford (1970) (see also Fig. 20). Such a comparison is rather subjective since it is often not easy to define a mean trend, especially at high galactic latitudes where fewer stars have been observed. Also, visual impressions depend on the used projection. However, the mean direction of region A1 ($170° \leq \alpha \leq 220°$) appears completely different from the galactic trend. Unfortunately nothing similar can be said about region A3 ($320° \leq \alpha \leq 360°$) due to the large dispersion of polarization vector orientations in the corresponding region of the Galaxy. Only a few (~ 5) quasars in the right part ($\alpha \geq 200°$) of the low-redshift region of alignments A2 (cf. Fig. 5) seem to have polarization vectors in the same direction as those of nearby stars, suggesting that their polarization could be of galactic origin. This region roughly corresponds to the North Polar Spur (Mathewson & Ford 1970, Berkhuijsen 1973). In fact, the small, moderately significant, excess seen in the first bin of one of the histograms of Fig. 19 ($d \geq 400$ pc) is due to these objects.

Statistical tests support this apparently weak contamination by instrumental and interstellar polarization. As expected, when the tests are applied to the sample of 150 galactic stars with $d \geq 400$pc and $|b_{II}| \geq 30°$, local deviations from uniformity are detected in 2D with a high significance. In fact, for $10 \leq n_v \leq 20$, $Z_c^m \simeq 6$ and S.L. is unresolved with 5000 simulations. Considering therefore the values of Z_c^m, one obtains a slightly better significance when angles are projected in galactic coordinates than in equatorial ones. On the contrary, for our sample of 170 quasars, the tests run in 2D (Fig. 15) do not detect anymore the significant effect observed in 3D, whatever the adopted coordinate system. Furthermore, neither the Celestial Pole nor the Galactic Pole correspond to a maximum of significance in Fig. 17, in agreement with the idea that the orientation effect is not due to an instrumental bias nor to a contamination by our Galaxy.

All these arguments concur to indicate that the observed polarization vector alignments are not likely to be an artefact due to instrumental polarization, or to result from interstellar polarization in our Galaxy. Since most knowledge of polarization by our Galaxy is from stars which, although distant, belong to it, one could invoke a different behavior of polarization in some remote regions of our Galaxy, or some unknown mechanisms. But even in this case it would be difficult to explain the redshift dependence of the observed alignments. We may therefore conclude that the observed alignments of quasar polarization vectors are most probably of extragalactic origin.

7.2. Are the alignments of cosmological origin?

The observed alignments of quasar polarization vectors may reflect an intrinsic property of the objects, or reveal a mechanism

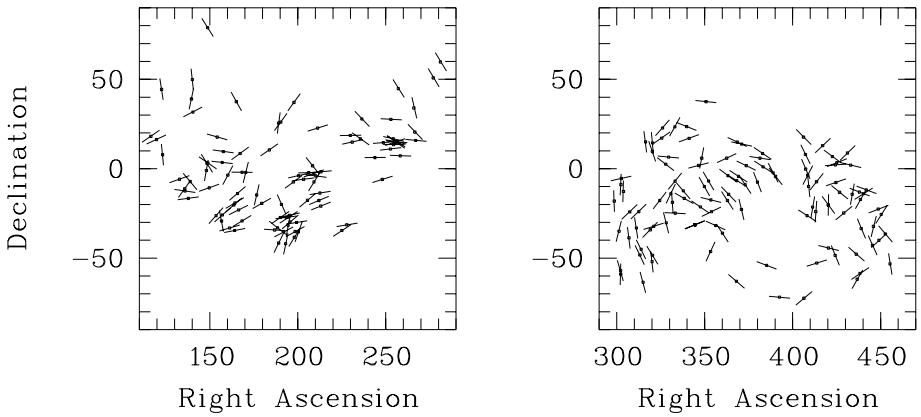

Fig. 20. Maps of galactic star polarization vectors projected in the equatorial coordinate system (right ascensions are in degrees). Data are from the Axon & Ellis (1976) catalogue. Only those stars with $d \geq 400$ pc and $|b_{II}| \geq 20^\circ$ are represented

which affects light on its travel towards us. The fact that they are observed at high redshift, with different or no counterpart at lower redshift, indicates the existence of correlations in objects or fields on very large spatial scales; the fact that they are spatially delimited suggests that this is not a global effect at the scale of the Universe. The orientation effect is observed independently of the nature of the objects: it concerns both radio-quiet and radio-loud quasars, as well as BAL, high or low polarization objects. Let us recall that for at least part of our sample, polarization angles are related to the morphological axis of the objects, indicating that the bulk of polarization should originate in the quasar themselves.

Several mechanisms may affect light as it propagates through the Universe, the most simple naturally producing polarization vector alignments being dichroism, or selective absorption. As far as we know, the only known mechanism of this type is extinction by aligned dust grains, which could be located in galaxies along the line of sight (Webster et al. 1995, Masci & Webster 1995). For the intervening galaxies to act as analysers, one would require rather precise coherent orientations of their axis on large scales, but also a fine tuning between the original quasar polarization and the extinction in the galaxies. Moreover, one would expect strong reddening, which is certainly not true for the optically selected objects. Other light propagation effects rely on optical activity, or circular birefringence, which produces a rotation of the plane of polarization. The most common is the well-known Faraday rotation which essentially works at radio wavelengths, being proportional to the square of the wavelength. Possible mechanisms based on anisotropic cosmologies, interactions with cosmic strings, vortices or pseudoscalar fields have also been proposed, and some of them already ruled out (Brans 1975, Manohar 1988, Harvey & Nakulich 1989, Carroll et al. 1990, Carroll & Field 1991, Harari & Sikivie 1992, Masperi & Savaglio 1995). In general, if one starts with a random distribution of polarization vectors, rotation effects are unable to produce alignments. However, within regions permeated by some cosmic magnetic field, the polarization vectors may oscillate between their initial direction and that related to the field (Harari & Sikivie 1992) such that, on the average, the polarization vectors could appear coherently oriented. Interestingly enough, a small amount of dichroism is also expected in this case, through the conversion of photons into pseudoscalars. Such an effect would scramble but not completely wash away the correlation between polarization angles and morphological axes (which is not so tight indeed). Although it is far from clear whether this mechanism can work on the observed scales, it is also difficult on the observational point of view to explain why objects at higher redshifts along the same line of sight do not have accordingly aligned polarization vectors, and why alignments with different mean directions exist along the same line of sight (cf. regions A1 & A2). This remark indeed applies to every effect based on light propagation.

On the other hand, we may admit that the quasars themselves, i.e. their structural axes, are coherently oriented on large spatial scales, in agreement with the observed correlation between object structure and polarization. In this case, one must seek for a mechanism acting at the epoch of formation, like for example those proposed to explain the possible alignments of galaxy rotation axes in nearby clusters, although the latter phenomenon, still controversial, refers to much smaller scales (MacGillivray et al. 1982, Djorgovski 1987, and references therein). Coherent orientations of structural axes may provide evidence for a weak cosmological magnetic field (Reinhardt 1971). Although speculative, such a scenario could more naturally account for the different local behaviors and mean directions. Note that the correlation between structure and polarization angles is only established for some quasars of our sample, and not necessarily for those quasars which participate to an alignment (there are not enough measurements for the latter objects).

It is important to specify that the correlation between structural axes and polarization vectors which seems valid for most quasars (including BL Lac objects) arises between the *optical* polarization vector and the *core* structural axis as measured on milli-arcsecond (VLBI) scale, these two quantities being apparently always aligned (Rusk 1990, Impey et al. 1991). Larger (VLA) structures compared to optical polarization vectors show a bimodal distribution, with alignment for the low polarization quasars and anti-alignment for the highly polarized ones (Moore & Stockman 1984, Rusk 1990, Berriman et al. 1990). Bimodal distributions are also observed when radio polarization vectors and VLBI structure axes are compared (BL Lac objects

included), when radio polarization vectors and VLA structure axes are compared, and also when radio-galaxies are considered (Clarke et al. 1980, Rusk 1987, Rusk 1990, Cimatti et al. 1993, and references therein). These properties and the fact that the optical and radio polarization angles of quasars are weakly or not correlated (Rusk & Seaquist 1985, Impey & Tapia 1990, Rusk 1990) may explain why no deviation from uniformity has been reported in the distribution of radio polarization angles for samples mixing quasars and radio-galaxies[3] (Bietenholz 1986). Furthermore, since in the framework of unification models (e.g. Antonucci 1993, Urry & Padovani 1995), radio-galaxies are thought to be identical to quasars but differently oriented, it is not excluded that coherent orientation effects cannot be detected for these objects.

8. Conclusions and final remarks

In the present study, we find that the optical polarization vectors of quasars are not randomly distributed over the sky as naturally expected, but appear coherently oriented on very large spatial scales. Statistical tests indicate that this effect is significant.

This orientation effect appears spatially delimited in 3D, typically occuring in groups of 10-20 objects; apparently, not all quasars have aligned polarization vectors. The fact that the polarization vectors of objects approximately located along the same line of sight are not accordingly aligned constitutes a very important observational constraint. However, since only small numbers of objects with different redshifts can be found exactly in front of the regions of interest, especially at higher redshifts, it would be worthwhile to confirm this result with additional polarimetric observations. The orientation effect itself could be confirmed independently by obtaining new measurements for other quasars located in the identified regions of alignments, the preferential direction of polarization vectors being predicted. The data could then be analysed with simple binomial statistics (as in Sect. 2), with the advantage that the objects contributing to the significance correspond to those visually identified without any ambiguity.

Since instrumental bias and contamination by interstellar polarization in our Galaxy are apparently unlikely to be responsible for the observed effect, the very large scale at which it is observed suggests the presence of correlations in objects or fields on spatial scales $\sim 1000\,h^{-1}$ Mpc at redshifts $z \simeq$ 1-2, h being the Hubble constant in units of 100 km s^{-1} Mpc^{-1}. Although more objects are needed to determine the scale accurately, this is more comparable to the size of the Cosmic Microwave Background anisotropies detected by COBE (Smoot et al. 1992) than to the largest structures detected so far from galaxies or from quasar absorption line systems ($\lesssim 150\,h^{-1}$ Mpc, Einasto et al. 1997, Quashnock et al. 1996).

[3] We confirm the absence of deviation from randomness also in 3D by applying our statistical tests to approximately the same data set, i.e. a sample of $\sim$ 300 objects with known redshift from Simard-Normandin et al. 1981. But one should notice that the redshift distribution is quite different from that in our sample, with significantly more objects at lower redshifts

No definite interpretation exists for this orientation effect, given the data. Since polarization angles are apparently correlated to structural axes, it is tempting to admit that the objects themselves are coherently oriented, suggesting a primordial origin. However, it is not clear at all that this correlation is valid for those quasars with aligned polarization vectors. In order to check this, it would be worthwhile to obtain VLBI data for them, and to see if the structural axes are also coherently oriented. Furthermore, it will certainly be interesting to know if the different classes of objects (quasars, radio-galaxies, BL Lac objects, etc) behave similarly, or not.

Whatever its origin, this new effect, if confirmed, may be of great interest for cosmology, especially since different interpretations are subject to direct observational tests.

Acknowledgements. I am indebted to E. Gosset and M. Remy for many enlightning discussions on statistical methods. E. Gosset, H. Lamy, M. Remy, and J. Surdej are acknowledged for their remarks on the manuscript, as well as the referee for his careful reading and constructive comments. I also thank J.F. Claeskens and L. Querella for discussions on cosmological models. E. Gosset is acknowledged for providing me with his Kuiper test code, and V. Mortiaux for encoding the data from Simard-Normandin et al. The NASA Astrophysics Data System (ADS) has been consulted. The catalogue of Axon & Ellis has been retrieved in electronic form thanks to the Centre de Données Stellaires (CDS) in Strasbourg, France. This research is supported in part by contract ARC 94/99-178

References

Antonucci R. 1993, ARA&A 31, 473
Arsham H. 1988, J. Appl. Stat. 15, 131
Axon D.J., Ellis R.S. 1976, MNRAS 177, 499
Bennett C.L., Banday A.J., Górsky K.M. et al. 1996, ApJ 464, L1
Berdyugin A., Teerikorpi P. 1997, A&A 318, 37
Berkhuijsen E.M. 1973, A&A 24, 143
Berriman G., Schmidt G.D., West S.C., Stockman H.S. 1990, ApJS 74, 869
Bietenholz M.F. 1986, AJ 91, 1249
Bietenholz M.F., Kronberg P.P. 1984, ApJ 287, L1
Birch P. 1982, Nat 298, 451
Brans C.H. 1975, ApJ 197, 1
Burstein D., Heiles C. 1982, AJ 87, 1165
Carroll S.M., Field G.B., Jackiw R. 1990, Phys. Rev. D 41, 1231
Carroll S.M., Field G.B. 1991, Phys. Rev. D 43, 3789
Cimatti A., di Serego Alighieri S., Fosbury R.A.E., Salvati M., Taylor D. 1993, MNRAS 264, 421
Clarke D., Stewart B.G. 1986, Vistas in Astronomy 29, 27
Clarke J.N., Kronberg P.P., Simard-Normandin M. 1980, MNRAS 190, 205
Cohen M.H., Ogle P.M., Tran H.D. et al. 1995, ApJ 448, L77
de Diego J.A., Kidger M.R., Pérez E., Takalo L.O. 1994, ApJ 424, 76
di Serego Alighieri S. 1989, 1^{st} ESO/ST-ECF Data Analysis Workshop, Grosbøl P.J. et al. (eds), 157
Djorgovski S. 1987, in Nearly Normal Galaxies, Faber S.M. (ed.), Springer-Verlag New-York, p. 227
Dressler A., Shectman S.A. 1988, AJ 95, 985
Einasto J., Einasto M., Gottlöber S. et al. 1997, Nat 385, 139
Fisher N.I. 1993, Statistical Analysis of Circular Data, Cambridge University Press, Cambridge

Harari D., Sikivie P. 1992, Phys. Lett. B 289, 67
Harvey J.A., Nakulich S.G. 1989, Phys. Lett. B 217, 231
Hawley D.L., Peebles P.J.E. 1975, AJ 80, 477
Hiltner W.A. 1956, ApJS 2, 389
Hutsemékers D., Lamy H., Remy M. 1998, in preparation
Impey C.D., Lawrence C.R., Tapia S. 1991, ApJ 375, 46
Impey C.D., Malkan M.A., Webb W., Petry C.E. 1995, ApJ 440, 80
Impey C.D., Tapia S. 1990, ApJ 354, 124
MacGillivray H.T., Dodd R.J., McNally B.V., Corwin Jr H.G. 1982, MNRAS 198, 605
Manohar A. 1988, Phys. Lett. B 206, 276
Masci F.J., Webster R.L. 1995, PASA 12, 146
Masperi L., Savaglio S. 1995, Astroparticle Phys. 3, 209
Mathewson D.S., Ford V.L. 1970, Mem. R. Ast. Soc. 74, 139
Moore R.L., Stockman H.S. 1984 ApJ 279, 465
Quashnock J.M., Vanden Berk D.E., York D.G. 1996, ApJ 472, L69
Reinhardt M. 1971, Ap&SS 10, 363
Rusk R. 1987, in The Impact of VLBI on Astrophysics and Geophysics, Reid M.J. & Moran J.M. (eds.), IAU Symposium 129, Reidel Dordrecht, p. 161
Rusk R. 1990, J. R. Astron. Soc. Can. 84, 199
Rusk R., Seaquist E.R. 1985, AJ 90, 30
Saikia D.J., Salter C.J. 1988, ARA&A 26, 93
Scaramella R., Baiesi-Pillastrini G., Chincarini G., Vettolani G., Zamorani G. 1989, Nat 338, 562
Simard-Normandin M., Kronberg P.P., Button S. 1981, ApJS 45, 97
Smith P.S., Schmidt G.D., Jannuzi B.T., Elston R. 1994, ApJ 426, 535
Smoot G.F., Bennett C.L., Kogut A. et al. 1992, ApJ 396, L1
Stockman H.S., Moore R.L., Angel J.R.P. 1984, ApJ 279, 485
Urry C.M., Padovani P. 1995, PASP 107, 803
Wardle J.F.C., Kronberg P.P. 1974, ApJ 194, 249
Webb W., Malkan M., Schmidt G., Impey C.D. 1993, ApJ 419, 494
Webster R.L., Francis P.J., Peterson B.A., Drinkwater M.J., Masci F.J. 1995, Nat 375, 469
Wills B.J., Wills D., Breger M., Antonucci R.R.J., Barvainis R. 1992, ApJ 398, 454

This article was processed by the author using Springer-Verlag LaTeX A&A style file *L-AA* version 3.